

SORPTION STUDIES OF OLIGONUCLEOTIDE DNA ON MONTMORILLONITE
CLAY: DEVELOPMENT OF AN IMPROVED ASSAY PROTOCOL

Presented to the Graduate Council of
Texas State University-San Marcos
in Partial Fulfillment
of the Requirements

for the Degree

Master of SCIENCE

by

Michael H. Robson, B.S.

San Marcos, Texas
August 2009

ACKNOWLEDGEMENTS

This work is dedicated to all who have supported this effort. First and foremost, to God, for with his blessings and grace anything is possible. Dr. Gary Beall, whom I have come to admire so much; I stand in awe at all you have accomplished and have taken on in your professional life. I will do my best to emulate your success. To Dr. Kevin Lewis, for it was in your lab that I was mentored and guided along. Thank you for your patience and dedication in transforming me into a scientist and training my mind to think as one. It was a pleasure to work under you and to get to know you. I would also like to mention all the faculty members that shaped my journey. You have all left an impression on me that I will not soon forget. I must thank Rachel Roberts, who served as mentor in the beginning and remained a friend throughout. Best of luck to you and I wish you the success that I know will come to you. Chris Lee, Jennifer Summers, Cory Holland, and all of the others that have been a part of the Lewis lab team, it was great to work with all of you. Thank you to my friends and classmates that I have met along the way. You have all made the past two years exciting and fun instead of an arduous process of necessity. I would be remiss not to thank my mother and father who have never wavered in their support of this endeavor. Thank you for the encouragement and reaffirmation that was sometimes needed along the way. My brother, Marc, you have always been a steadfast supporter of my dreams and have always been there to help keep my life in perspective. And most of all, thank you to my beautiful wife, Lacie. Without you I may have never strived for something like this. You are the one that keeps me grounded in what is truly important in

life and I know that you will always be there to remind me when I stray. You are the one that gives me the motivation and desire to reach higher, and I thank you for coming with me on this journey.

TABLE OF CONTENTS

	Page
ACKNOWLEDGEMENTS.....	iii
LIST OF TABLES.....	vi
LIST OF FIGURES	vii
CHAPTER	
I. INTRODUCTION	1
II. MATERIALS AND METHODS.....	13
III. RESULTS AND DISCUSSION	20
REFERENCES	68

LIST OF TABLES

TABLE	Page
1. Fractions of Na and Ca Montmorillonite that are Resistant to Precipitation by High-Speed Centrifugation in Unsonicated Aqueous Solutions.....	27
2. Impact of Sonication on Sedimentation of Na and Ca Montmorillonite Clays.....	29
3. Analysis of Residual Clay After Filtration of Na Montmorillonite	34
4. Impact of Na and Mg Counterions on Binding of Single-Stranded Oligonucleotide DNA to Sonicated Homoionic Na Montmorillonite ^a	39
5. Impact of Na and Mg Counterions on Binding of Single-Stranded Oligonucleotide DNA to Sonicated Homoionic Ca Montmorillonite ^a	40

LIST OF FIGURES

FIGURE	Page
1. Cross Section of a Clay Platelet.....	3
2. Model of the Atomic Structure of a Montmorillonite Clay Platelet	4
3. Representation of Polymers Associating With Clay Platelets	6
4. Computer Model of a DNA Molecule Intercalating a Montmorillonite Clay Tactoid Gallery	6
5. The DNA Molecule.....	8
6. Absorbance Spectra of Various Substances.....	22
7. Absorbance of UV Light by Montmorillonite	24
8. Timed Sonication of Ca-Mont vs Absorbance at 230 nm.....	26
9. Plot of 100 °C Heating Times vs Absorbance at 230 nm and 450 nm	31
10. Comparison of $A_{230}:A_{450}$ Ratios.....	32
11. Effect of Salt on Sedimentation Efficiencies of Na Montmorillonite and Ca Montmorillonite	36
12. Plot of Percentage of DNA Bound to Clay vs Increasing Salt Concentration	41
13. New Binding Assay Method vs Previous Binding Assay Method	42
14. Agarose Gel with Single and Double Stranded 25-mer DNA	44
15. Computer Model of Single-Stranded DNA Intercalated Within a Na Montmorillonite Tactoid	48
16. Absorbance Scans of Heated Na and Ca Montmorillonite	50
17. Absorbance Scan of ddH ₂ O Before and After Heating in a Microfuge Tube	51

18. Extended Spectrum Scans of ddiH ₂ O Heated in Ambion and VWR Microfuge Tubes	53
19. Absorbance Scans of ddH ₂ O Heated at Various Temperatures in Tubes	55
20. Absorbance Scans of ddH ₂ O Sonicated in Tubes	57
21. Absorbance Scans of Organic Solvents Heated in Tubes	59
22. Change in Absorbance of BSA and Salmon Sperm Chromosomal DNA from Heating in Tubes	61
23. Absorbance Scans of ddH ₂ O After Thermalcycling in PCR Tubes	62
24. Absorbance Scans of ddH ₂ O Heated in Various Brands of Tubes	64

CHAPTER I

INTRODUCTION

It has been proposed that clay minerals may have had a role in the origination of life on Earth. First postulated by John Desmond Bernal, he suggested that small molecules would bind to the clay surfaces, which would align them in such a way as to facilitate reactions (1). Not only could the clay catalyze the formation of small biomolecules, furthermore, the clay could protect the fragile molecules from degradation and decay from heat and photo-degradation because these molecules could reside in spaces in the clay. It is possible, therefore, that life on Earth owes a great deal to clay for providing the ideal conditions for prebiotic molecules to synthesize and expand into polymers such as polynucleotides (2).

Clay has also remained useful to organisms because of its role in lateral transfer of DNA between species. A competent bacterium can be transformed by the uptake of DNA found in clay, thereby expressing genes from a potentially unrelated organism (3-6). Bacterial evolution theorists hypothesize that clay has a major role in the evolution of bacteria for this reason (7). Although most experiments in bacterial transformation from DNA found in soils have been conducted in a laboratory under ideal conditions, it is apparent that this scenario can play out in nature. While new discoveries in the field of clay-DNA research are exciting, they are also somewhat alarming. Modern industry and agriculture use genetically modified organisms, and therefore it is vital to manage and

monitor altered organisms so as not to contaminate the gene pools of the natural environment with transgenic DNA that may be potentially destructive to the organisms or the human population. Although such an event seems somewhat like science fiction, it is a real concern that must be addressed, and more importantly, understood. Especially in the case of genetically engineered microorganisms where the majority of genetic alteration occurs, sensitive and thorough methods for detecting and containing the microbes must be developed to prevent uncontrolled propagation throughout the ecosystem.

Smectites are a well-researched group of naturally occurring ceramic clays, which are materials composed primarily of silica, alumina, Fe (II), Fe (III), and water. They will often incorporate a metal cation, most commonly Na^+ , K^+ , Ca^{2+} , Mg^{2+} , and Fe (II) (8). These clays form thin sheet-like layers that are about 1 nm thick and 200 – 1000 nm wide, which give them a high aspect ratio, thus qualifying them as nanomaterials (Figure 1) (9). Clays have a variety of unusual chemical and physical properties that have been exploited in several industries, including the automotive, cosmetic, food, and health fields (10, 11). In the presence of water, smectites undergo a large volume increase and are often referred to as “swelling” clays. Another property they possess is a high surface area to mass ratio due to their extremely thin and broad sheet structure. They have a high modulus, a high cation exchange capacity, and form stable dispersions in aqueous solutions (12, 13).

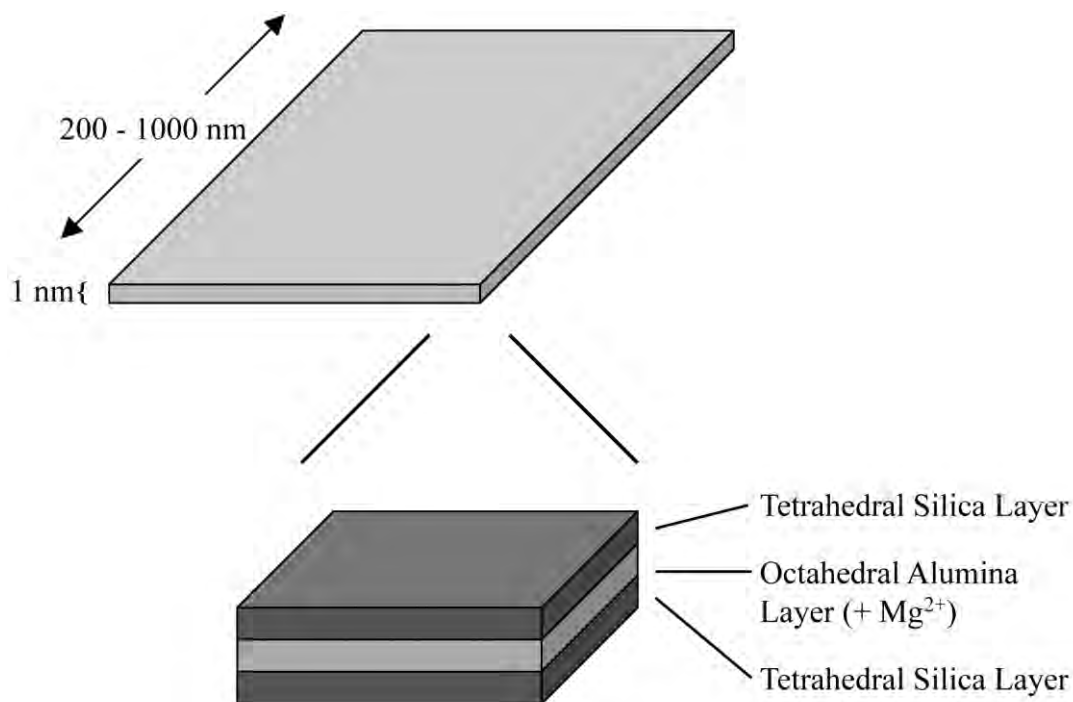


Figure 1. Cross section of a clay platelet that depicts the sheet-like planar dimensions as well as the laminar components of the platelet. Not shown are the cations that associate with the clay surfaces.

The clays form platelets that have a sandwich-like structure that consists of a positively charged octahedral core of alumina, oxygen, iron and some cations like Mg^{2+} , and is flanked on each side by a tetrahedral layer of silica lattice (SiO_4^{4-}) (Figure 2). The platelets have a monolayer of water adsorbed to the surface and the SiO_4^{4-} imparts upon these platelets an overall negative charge. The platelets stack upon one another in a turbostatic fashion so that they have no preference as to how they orient in relation to one another and form what is called a tactoid, much like a stack of pancakes (14, 15). Due to its large surface area and overall negative charge, the platelet can become saturated with adsorbed cations in the spaces, or galleries, between the sheets of the tactoid. The width

of the gallery depends on several factors, such as the type of exchangeable cation, degree of hydration, and the size of the intercalating species. Tactoid size is also affected by the cations that are present, where Ca^{2+} will facilitate the formation of larger tactoids than Li^{+} or Na^{+} (15-20).

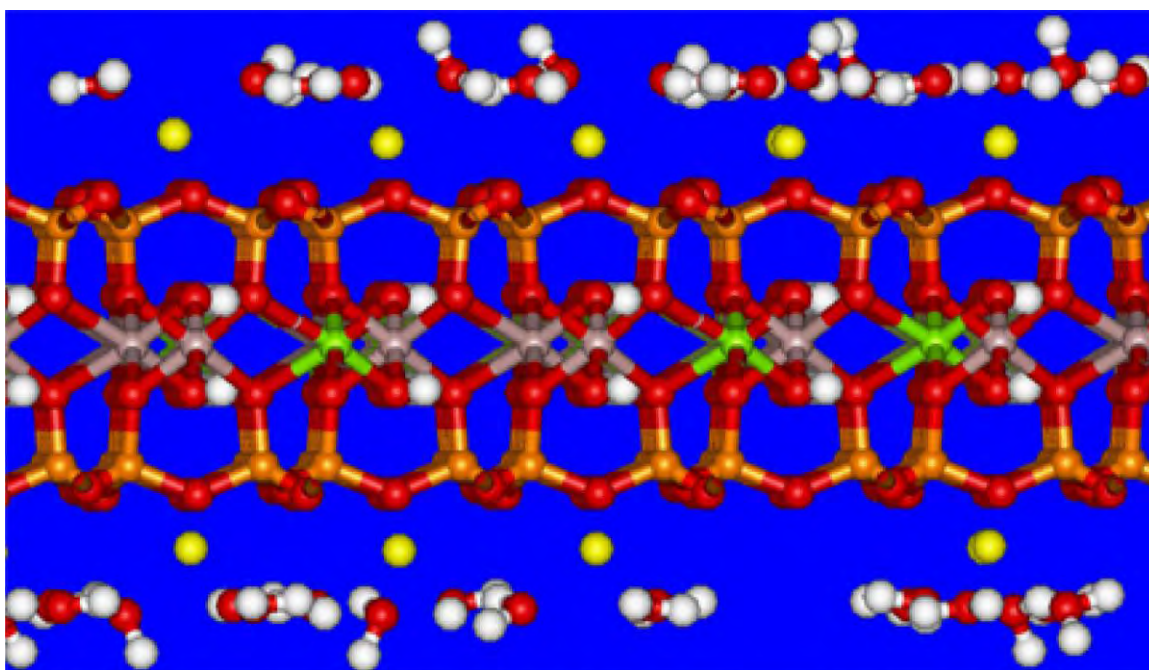


Figure 2. Model of the Atomic Structure of a Montmorillonite Clay Platelet. The tetrahedral silica layer can be seen in orange. The yellow atoms near the surface are positively charged cations that are attracted to the clay surface due to the presence of the electronegative oxygen molecules of the silica lattice.

The role of cations in the different clays has been studied (21). The absorption of UV light by hydrated clay is strongly affected by the presence of Fe (III) and is inversely affected by the size of the tactoid (16, 22). Montmorillonite clays exhibit absorption spectra with a broad-shouldered peak between 200 nm and 300 nm. Depending on the cation present, e.g., Ca^{2+} , Na^{+} , etc., the peak will vary in size and strength due to the tactoids that form (14). Slight variations also exist between varieties of clays such as

kaolinite, goethite, montmorillonite, and hectorite due to variances in structure and Fe (III) levels.

One unique characteristic of clay in the presence of cations is that charged organic polymers can adsorb to the clay surfaces in several proposed ways, which protects them from degradation (Figure 3) (23). The polymer can intercalate within the galleries of the tactoids (Figure 3A, Figure 4), cause the platelets to exfoliate randomly and adsorb to the individual platelets (Figure 3B), or adsorb to the exterior of a clay tactoid (Figure 3C). Adsorption of charged organic molecules to clay surfaces in the presence of cations has experimentally been shown to change with pH (24), cation type (25), temperature (26), and nature of the molecule being adsorbed (27). For example, DNA nucleotides adsorb to both Na^+ bound montmorillonite (Na-Mont) and Ca^{2+} bound montmorillonite (Ca-Mont); however they bind more readily to Ca-Mont than to Na-Mont (26). Furthermore, nucleotides adsorb better at both a lower pH and temperature than at a high one. Biomacromolecules such as proteins have also been shown to adsorb to clay, and are protected from environmental degradation. Synthetic polymers are also capable of binding and intercalation, thus forming clay:polymer nanocomposites, where the presence of the clay can enhance or drastically alter the properties of the polymer (8).

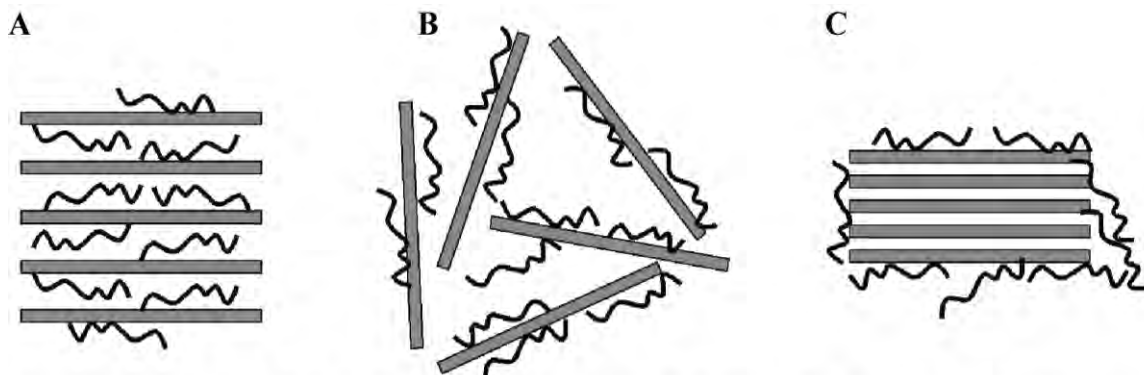


Figure 3. Representation Polymers Associating With Clay Platelets. Proposed ways in which polymers (black, crooked lines) may interact with the clay platelets (gray, thin rectangles) by (A) intercalating within the galleries of the tactoids, (B) exfoliation of the tactoids upon adsorption, or (C) by adsorbing to the outer surfaces of the tactoids.

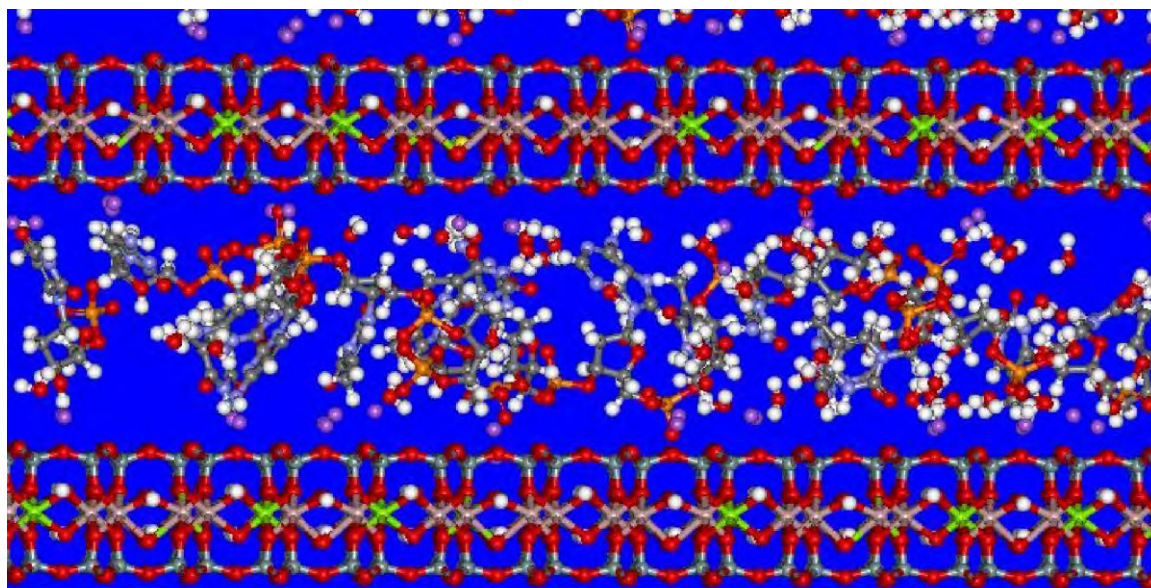


Figure 4. Computer Model of DNA Intercalating a Montmorillonite Clay Tactoid Gallery.

The presence of the cations is essential to the adsorption of biomolecules to clay surfaces (25). Montmorillonite clay is the preferred medium for the adsorption of such molecules; however in the absence of cations, nucleotides have been shown to be incapable of adsorption. It has been suggested that divalent cations are better mediators of

interaction with biomolecules, such as DNA, than monovalent cations. Altering concentrations of salts such as NaCl or MgCl₂ in the clay–DNA solution has an effect on the DNA molecule’s affinity for the clay surface, where higher concentrations improve DNA binding (6, 23, 25, 28).

Of the prior listed clays, montmorillonite has emerged as the preferred medium for clay adsorption studies since it is ubiquitous in nature. It has also been shown to be an effective facilitator in chemical reactions involving nucleotides converting to another form, or elongation of oligomers (29). It also adsorbs nucleotides when bound to Mg²⁺ better than kaolinite or goethite (23). When pH is lowered, as mentioned earlier, the adsorption of nucleotides increases. With the exception of goethite at pH 3.0, montmorillonite binds DNA better than the other varieties.

Some properties of the nucleotide are inherently intrinsic to adsorption while others are not (27). Although purines adsorb better than pyrimidines in their mononucleic form, polynucleotides base composition is not a factor in the interaction of the nucleotide and the clay surface, which would indicate that the bases do not interact with the cation bridge. In respect to linear DNA, the type of end on the polynucleotide has no effect either. Peitramellara, *et al.* (27) have shown that whether the end is blunt or has a “sticky” overhang, the exposed end bases exhibit no effect from the exposed positive charges, however this was done using an error prone assay. Mononucleotides adsorb at a lower rate than polynucleotides, but smaller polynucleotides adsorb better than larger ones. Supercoiled DNA (scDNA) has a lower affinity for adsorption than linear double-stranded DNA (dsDNA) and single-stranded DNA (ssDNA), an experiment, which was

conducted using a flawed assay, which will be addressed (22). A somewhat contradictory result is observed where chromosomal DNA, which is supercoiled, will adsorb more readily than plasmid DNA and RNA (30). The greatest contributing factor to DNA adsorbing to clay is the phosphate backbone, which provides an overall negative charge to the DNA molecule due to the concentration of electronegative oxygen atoms (Figure 4) (31). Therefore the probable mechanism by which the DNA (or nucleotide) adsorbs to the clay surface is through an organic ligand (32), such as phosphate or citrate, or more likely, a cation bridge. This is where the cation binds to the surface of the clay, which has an overall negative charge, and the DNA will in turn attach itself to the

cation and not come into physical contact with the clay. It has been proposed that the

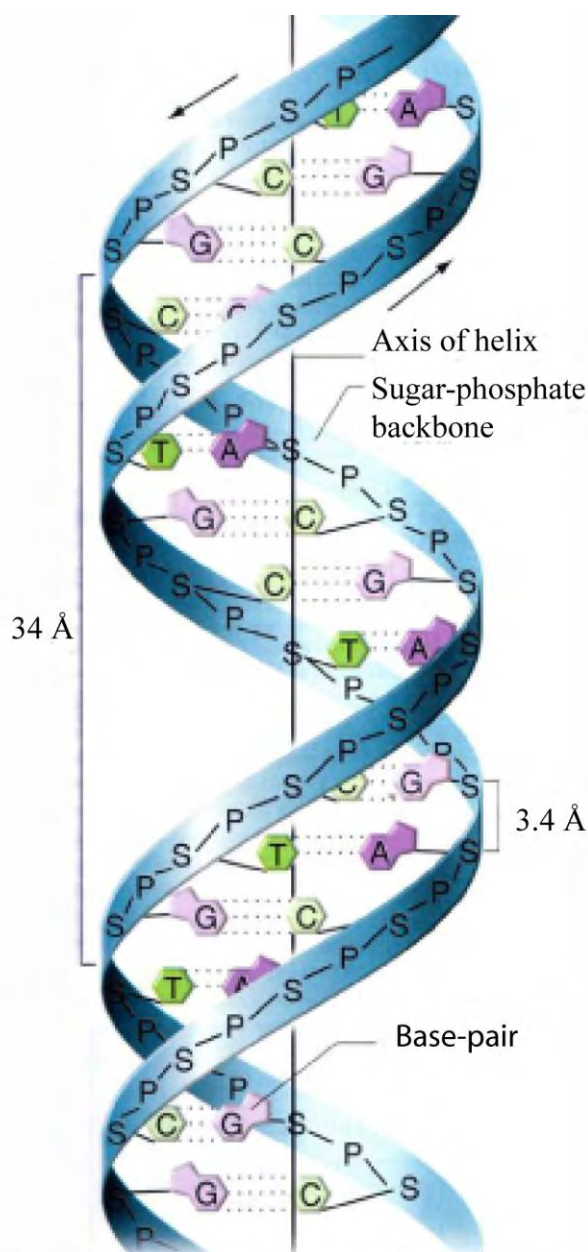


Figure 5. The DNA Molecule. Shown is the sugar-phosphate backbone, which has a negative charge density, is twisted into a double helix conformation. Bases can be seen pairing with their complements, where adenine (A) pairs with thymine (T), and cytosine (C) pairs with guanine (G).

DNA can interact with the octahedral lattice edges of the platelets where exposed Al^{3+} and Mg^{2+} resides, via the phosphates, but this is unlikely because the edges are primarily terminated with hydroxyls rather than cations and account for only about 2% of the total surface area of the clay (8,12).

Soils are rife with DNA, particularly with microfloral varieties like linear chromosomal DNA and supercoiled circular plasmid DNA, where they can reside for several months. Some DNA in soil is from plants, but most is from bacteria. These two types of DNA have different abilities to transform bacteria and also have different adsorption characteristics. Low Temperature Scanning Electron Microscopy (LTSEC) showed that plasmid scDNA aggregates into toroidal filaments, and sometimes web-like structures, which can be relatively long and thick in comparison to the clay platelets to which they adsorb (22). Linear dsDNA by contrast, may simply adsorb to the clay surface without aggregating with other DNA molecules. Ca^{2+} is the predominant cation in soil, and its electrostatic attraction to the DNA backbone neutralizes the negative charges, thereby reducing inter- and intrarepulsive forces in aqueous solution, which serves to compact the molecule. In one particular experiment, Poly *et al.* (22) showed that plasmid DNA was seen via LTSEM in an aggregate formation extending between the platelet edges. Conversely, the linear dsDNA adsorbed to both the clay surface and the edges.

As previously mentioned, clay can protect adsorbed DNA from degradation. In the presence of the polynucleotide degrading enzyme DNase I, bound DNA was protected from the activity of the enzyme (4, 6). In fact, it took 10 times the concentration of DNase I to inhibit the transformation of bacteria by DNA bound to clay than DNA free

in solution. Although DNase I is not found in high concentrations in soil, this experiment did demonstrate that clay has a stabilizing effect on the DNA and can protect it from an array of factors including UV light and X-rays. It should also be noted that sand will also adsorb DNA and it is hypothesized that silt and other earthen components will interact with DNA in much the same way (6). This may provide an explanation for the presence of cryptic genes found in bacteria in the form of plasmids. These genes appear in bacteria taken from soil samples and appear to have no protein expression in the host cell.

The characteristics of clay make it an ideal material for the delivery of genes to a target cell for gene therapy (33, 34). Due to its stable and non-toxic nature, coupled with its ability to tightly adsorb and protect biomolecules from enzyme and photocatabolic degradation, montmorillonite may be essential to the future of healthcare by its employment in vital therapeutic techniques. Researchers have demonstrated that clay can protect a vector containing the gene for green fluorescent protein (GFP) from the hostile environment of the stomach and digestive tract to ultimately being expressed in the intestines of mice (33). Expression of GFP is a precedent for further investigation into delivery vectors for gene therapy, and this technique may revolutionize this approach to alleviating genetic illness. In order to better understand how clay accomplishes this, we must further investigate the relationship that clay has to DNA in these complexes to optimize efficiency for gene delivery.

In most quantitative studies of the interaction of DNA and clay, the two materials were mixed together in an aqueous solution in the presence of a metal cation and the affinity of the DNA for the clay was measured using the same basic process (3-6, 22-27,

30, 32, 34, 35). Clay, sometimes dispersed by sonication but mostly not, was already associated with a cation and had been mixed into solution. DNA was then added to the solution, given time to adsorb, and the mixture was subsequently centrifuged. The supernatant was decanted and the remaining pellet assumed to contain all of the clay and any adsorbed DNA. To measure the concentration of unadsorbed DNA, the supernatant was tested for absorption of UV light at 260 nm, the peak of absorbance for nucleic acids. At that point a simple subtraction would reveal how much DNA had adsorbed to the clay. Using this process as a framework for experiments, variables such as types and concentrations of metal cations, pH, DNA structure, and clay type can be tested.

Researchers will often employ polyolefin plastics, which are commonly used polymers because of their low production costs and the fact that they can both protect and resist the contents of the container that they have been used to make. The majority of researchers in the field of biochemistry use polypropylene microfuge tubes to conduct experiments. Such experiments include routine purification, denaturation, and long-term storage of DNA, RNA, and proteins. Additionally, most enzyme-catalyzed reactions are performed in polypropylene tubes, which range in capacity from 0.2 mL to 2.0 mL. These ubiquitous tubes are inexpensive, convenient, and able to withstand the rigors of experimentation, including, but not limited to, heating, freezing, high g-force centrifugation, harsh solvents, and sonication. Large-scale production of commercial polyolefins requires the addition of stabilizers in order to retain their physical, mechanical, and chemical properties during the production process as well as under the conditions of their intended use (36). Fabrication of polypropylene tubes involves

liquefied polymer being forced into an injection mold and stabilized with mold release agents and antioxidants. The stabilizers used are manufacturer-dependent, but some common additives are pentaerythrityl tetrakis (3,5-di-*tert*-butyl-4-hydroxyphenyl) propionate (Irganox 1010), tris (2,4-di-*tert*-butylphenyl) phosphate (Irgafos 168), and benzophenone (37, 38). Many stabilizers act as reducing agents to atmospheric O₂ under extreme conditions in order to protect the polymer from degradation, and in doing so are degraded into smaller species. The degraded antioxidants have been known to migrate, or leach, from the polypropylene plastic (39). Some of the compounds that migrate out of the plastic material are of concern, for both health and experimental reasons, such as bisphenol A, which is a known “endocrine disrupter” (40).

The primary goal of this project was to analyze the associations of DNA molecules with clay particles using new investigative approaches, and develop a protocol for an assay that would correctly measure this DNA. These experiments have led to the discovery of a persistent error in all previous applications of methods involving centrifugation to quantify DNA bound to clay. In the course of this project, another unforeseen factor emerged in the quantification of DNA and other biomolecules. Plastic materials found in laboratories everywhere, and common to enclosed vessels, have been found to leach derivatives into the contained solution. Our project has established the additional goal of documenting the conditions and the degree to which a variety of plastic tube types from a myriad of manufacturers release these chemicals. We also have analyzed the effects that this “leachate” has, especially with UV spectroscopy due to its universality in biochemical laboratories.

CHAPTER II

MATERIALS AND METHODS

I. MATERIALS

General Reagents

Dimethyl sulfoxide (DMSO) and magnesium chloride (MgCl_2) were purchased from Sigma Chemical Co. (St. Louis, MO). Acetone, chloroform, methanol (MeOH), and sodium chloride (NaCl), were provided by Fisher Scientific (Fair Lawn, NJ). Anhydrous diethyl ether was furnished by J.T. Baker (Phillipsburg, NJ). Autoclaved double deionized water (ddH_2O) was used in all experiments where water was used, and was made in the lab of Dr. Kevin Lewis. Agarose and ethidium bromide were supplied by Shelton Scientific, Inc. (Shelton, CT). Irganox 1010 and Irgafox 168 were supplied by Ciba (Basel, Switzerland).

Clays

Powdered homoionic sodium montmorillonite (Na-Mont) and calcium montmorillonite (Ca-Mont) were obtained from Southern Clay Products, Inc. (Gonzalez, TX). For the majority of experiments involving clay, stock solutions were used that were made at either 2 mg/mL or 5 mg/mL. The solutions were made using double-deionized water (ddH_2O) followed by a thorough mixing by vortex. Stock solutions were further

differentiated by sonication, a method described in detail in the Methods section. Na-Mont was sonicated for 5 min and Ca-Mont was sonicated for 10 min.

Deoxyribonucleic Acid and Protein

Pvu4a 25-mer oligonucleotide DNA and its complement, cPvu4a, were synthesized by BioServe BioTechnologies Ltd. (Beltsville, MD). dsDNA was prepared by annealing Pvu4a and cPvu4a in solution by mixing equal concentrations of each with or without 10 mM MgCl₂ and heating to 95 °C, and subsequently cooling the solution to room temperature. Annealing was confirmed by gel electrophoresis. Salmon sperm chromosomal DNA was purchased from Invitrogen Life Technologies (Carlsbad, CA). Purified Bovine Serum Albumin (BSA) and 50 base pair DNA standard were provided by New England BioLabs (Beverly, MA).

Oligomer Sequences:

Pvu4a: 5'-AAATGAGTCACCCAGATCTAAATAA-3'

cPvu4a: 5'-TTATTTAGATCTGGGTGACTCATTT-3'

Microfuge Tubes, PCR Tubes and Pipetman Tips

The Polymerase Chain Reaction (PCR) tubes, all 0.2 mL, were used only for the polypropylene leachate studies. For the purpose of these experiments, several tubes from different manufacturers were selected and are as follows: Ambion AM12225 PCR Tubes, Ambion (Austin, TX) now part of Applied Biosystems; Labcon PCR tubes (VWR catalogue #) 21070-012, Labcon (San Francisco, CA), now part of VWR International,

Inc.; Genunc 250865 PCR tubes from Nalgene of Thermo Fisher Scientific (Rochester, NY); VWR 20170-010 PCR tubes, VWR International, Inc (West Chester, PA); Gene Mate Ultra Flux Dome Cap PCR tubes C-3257-1, by ISC Bio Express (Kaysville, UT)

A variety of standard 1.5 mL or 0.6 mL microfuge tubes from several manufacturers were used. The only 0.6 mL microfuge tube was the AM 12300 Microfuge Tube from Ambion (Austin, TX). The 1.5 mL microfuge tubes selected for use were AM 12400 microfuge tubes by Ambion (Austin, TX), MCT-175-A and MCT-150-C microfuge tubes from Axygen Scientific (Union City, CA), and 20170-038 microfuge tubes for High G-Force from VWR International, Inc (West Chester, PA). This VWR tube was the microfuge tube of choice in the majority of the polypropylene leaching studies, with tubes from multiple batches having been tested. The Ambion 12400 Microfuge tube was used in most studies involving clay. The 245107 1.5 mL microfuge tube by Eppendorf (Westbury, NY), the 02-681-376 1.5 mL tube from Fisherbrand, a.k.a Fisher Scientific (Fair Lawn, NJ), and the 72.694 1.5 mL microfuge tube from Sarstedt (Numbrecht, Germany) were also tested for leaching.

Two 2.0 mL microfuge tubes were tested as well in the polypropylene leaching studies. The 12425 microfuge tubes from Ambion (Austin, TX) and C-3261-3 micro-centrifuge tube by ISC BioExpress (Kaysville, UT) were used in these studies. Pipetman tips used in all experiments were also tested for polypropylene leaching in the presence of solvent. BioLogix (Shawnee Mission, KS) manufactured the BPT-1000BB 1000 μ L pipet tip, and Gentaur (Kampenhout, Belgium) made the 20-0200 non-sterile yellow pipet tip.

II. Methods

Gel Electrophoresis

Gel electrophoresis was performed using a 4.0% agarose gel prepared in TBE (90 mM tris-borate, 2 mM EDTA) running buffer in the Life Technologies (Now part of Applied Biosystems) (Foster City, CA) Horizon 11-14 gel rig at 110 V. The unusually high concentration 4.0% agarose was used to separate the bands of short length DNAs. Staining with ethidium bromide was done for 15 min followed by destaining for an additional 15 min in ddH₂O. The gel image was captured digitally with a Kodak IS440 CF Image Station, Kodak (Rochester, NY) with the assistance of the Kodak 1D imaging software.

Ultraviolet (UV) Spectroscopy

UV Spectroscopic scans and measurements were performed using a BioRad (Hercules, CA) SmartSpec 3000 spectrophotometer, or on a few occasions the BioRad SmartSpec Plus spectrophotometer. Scans were conducted using the slow scan setting with the smoothing function activated for the scan print. A UV compatible BioRad TrUView ultramicro-cuvette or a standard 3.5 mL quartz cuvette were used for UV spectra measuring solutions in water. When an organic solvent was analyzed, the quartz cuvette was employed in measuring UV absorbance. Na-Mont and Ca-Mont solutions were typically scanned at dilute concentrations of 0.2 or 0.3 mg/mL due to the high

optical density of the clay. DNA solutions were diluted to concentrations of approximately 77 $\mu\text{g/mL}$.

X-Ray Diffraction

Analysis using X-ray diffraction was performed using a Bruker (Madison, WI) AXS D-8 diffractometer, which was fitted with a Cu K α X-ray tube and a Solex detector. Glass slides were prepared by creating a solution of ddH₂O using S Na-Mont, U Na-Mont, S Ca-Mont, or U Ca-Mont in combination with or in the absence of Pvu4a DNA or its complement cPvu4a, and either 10mM MgCl₂ or 1M Tris buffer (pH 8.0). The sample was centrifuged at 18,000g at 20 °C for 20 min and the solution was subsequently decanted and the wet pellet was mounted on a slide and scanned from 1 to 20 degrees two theta with a step size of 0.05° and a 10 sec count time at each step.

Polymerase Chain Reaction

Polymerase Chain Reaction procedures were performed using the Applied Biosystems (Foster City, CA) 2720 Thermal Cycler. Although DNA was not amplified for the purposes of the research, the machine was run using PCR tubes from several manufacturers filled with 150 μL ddH₂O. The machine was run for 30 cycles using the following parameters: 95 °C for 2 min, followed by 30 cycles involving 95 °C for 45 sec, 60 °C for 30 sec, 72 °C for 2 min. The tubes were then incubated at 72 °C for 7 min and placed at 4 °C until removed from the cycler.

Centrifugation

Centrifugation was used to sediment clays from solution and, in separate experiments, to induce stress onto microfuge tubes to study leaching of polypropylene additives. Three different centrifuges were used to conduct these experiments. Most commonly used was the Eppendorf Centrifuge 5415D (Westbury, NY) operated at 13,200 RPM and 16,100g. A Beckman Coulter (Fullerton, CA) Microfuge 18 Centrifuge, which was rotating at 14,000 RPM and 18,000g. High g-force centrifugation was achieved using the floor model J2-21 Centrifuge by Beckman (Now Beckman Coulter, Fullerton, CA) with the Beckman JA-25.50 rotor spun at 14,000 RPM and 19,756g and cooled to 20 °C.

Sonication

The majority of sonications of clay solutions were achieved using the Sonics & Materials, Inc. (Newtown, CT) Vibracell VC130 Sonicator in Dr. Lewis' lab. The amplitude of the sound waves was slowly increased manually to the 30 mark and sustained for the duration of the sonication. In early experiments, clay solutions were sonicated using the Sonics & Materials, Inc. Vibracell VC501 with the 3 mm probe at an amplitude of 40. Sonication times ranged from 30 sec to 20 min. Solutions of clay in ddH₂O were sonicated on a larger scale, using 50 mL tubes that were fixed in place so that the probe was not in contact with the sides of the tube. The Vibracell VC501 in the lab of Dr. Beall was used in the sonication of initial stock solutions of clay.

Autoclaving

The Hiclave HV-50 by Hirayama (Saitama, Japan) was used to autoclave microfuge tubes for the purpose of analyzing the leachate. Microfuge tubes were immersed in ddH₂O in a flask so that they were submerged using the smallest ddH₂O volume:tube surface area ratio possible. The autoclave was set to the liquid phase (121 °C for min) and allowed to cool to room temperature upon completion.

CHAPTER III

RESULTS & DISCUSSION

Traditionally, the quantification of the adsorption of DNA to clay has been measured by mixing the two components, followed by centrifugation at high g-force and calculating the concentration of DNA left in the supernatant utilizing UV absorbance spectroscopy (3-6, 22-27, 30, 32, 34, 35). It was reasonably presumed in these studies that all clay particles would precipitate after centrifugation. This appeared to be a correct assumption because an aqueous solution of clay would in fact become clear to the naked eye, just like pure water. This assumption failed to account for the fact that nano-sized clay particles are small enough that no light refraction will occur and thus appear to be transparent. Quantification of unbound DNA in these studies was achieved by spectroscopically analyzing the supernatant for absorbance at 260 nm. Nucleic acids exhibit strong absorbance with a peak at 260 nm, which is the wavelength that is routinely used to monitor their concentration in solution. Homoionic clays and proteins will also absorb in this region of the spectrum (Figure 6). The absorption spectra of Fe (III) from aqueous FeCl_3 , Na-Mont, Ca-Mont, salmon sperm DNA, and Bovine Serum Albumin protein (BSA) are shown in Figure 6, A-E, respectively. The wavelength of maximum absorption of UV light is clearly defined. The peaks of interest are at 220 nm for BSA, 230 nm for Fe (III), Na-Mont, and Ca-Mont, and 260 nm for DNA, represented by salmon sperm DNA. The peak at 230 nm observed in Na-Mont and Ca-Mont is the direct result of the absorption of UV light from the Fe (III) in the lattice of the clay

platelet (16). Due to the overlap of the clay peak with the peak for nucleic acids, the absorbance of one substance will contribute to the measured absorption of the other component in a mixture if both are present. This phenomenon is due to the peaks having strong absorption in the shoulders at the point of overlap. This overlap will have an additive effect on contribution to absorption of a mixture of clay and DNA in solution if the clay is not sedimented completely in a centrifugation experiment.

Montmorillonite clay commonly occurs in nature in mixed ionic form that contains mainly sodium and/or calcium as the exchangeable cation. The dispersion and absorption characteristics of these two ionic forms are quite different, as will be discussed below.

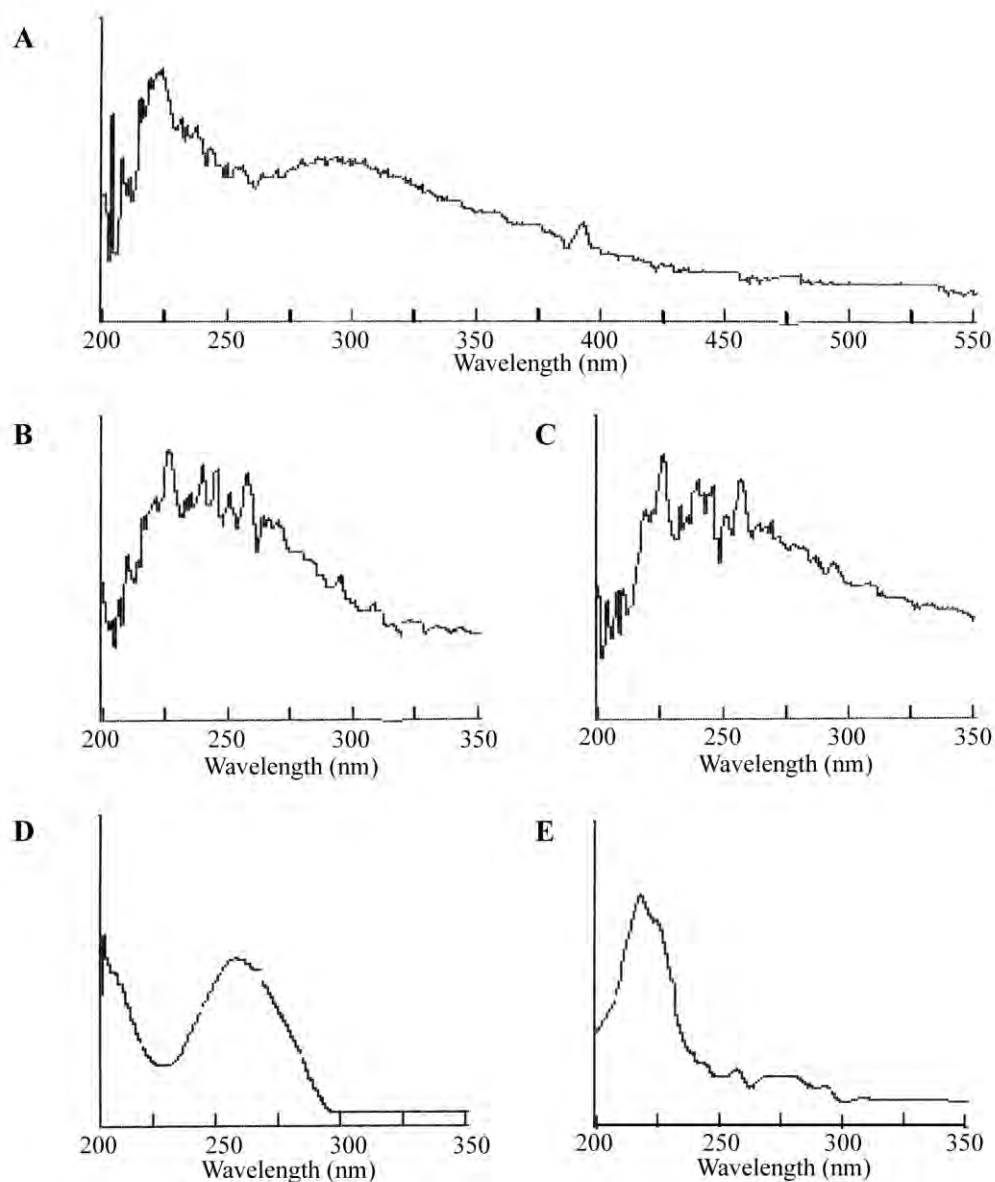


Figure 6. Absorbance Spectra for Various Substances. Aqueous solutions using ddH₂O have maximum peaks for (A) Fe(III) from $\text{FeCl}_3(\text{aq})$ at 224 nm, (B) Na Montmorillonite and (C) Ca montmorillonite uncentrifuged clay solution at 230 nm, (D) chromosomal salmon sperm DNA at 259 nm, and (E) Bovine Serum Albumin at 220 nm.

Absorption of UV light at the peak wavelength of 230 nm is directly proportional to the concentration of clay. This absorption can be strongly affected by sonication. Sonication is a technique that is employed in clay research to break up and disperse the tactoids of clay platelets whereby ultrasonic waves are created in the solution, which creates heat and violent cavitation of the local environment. The combination of heat and cavitation scatters the platelets and may even break covalent bonds within some of them in the process, potentially exposing even more Fe (III) from within the silica lattice. Dispersion of clay is essential to the formation of clay:polymer nanocomposites to increase the available surface area for the polymer to associate with the clay. The effect of sonication on clay can be readily observed with a quick, visual study of the sedimentation of clay solutions in a glass bottle by shaking it up and watching the clay sediment. Sonicated clay stays suspended much longer in relation to the unsonicated clay of the same type, especially in Ca-Mont solutions. Contributions from Rachel Roberts and Drew Sowersby in their undergraduate research discovered an additional effect. While the absorbance of Na-Mont doesn't significantly increase with sonication as concentration is increased, Ca-Mont exhibits a drastic change in absorbance at 230 nm (Figure 7) (41). While sonication increases the absorbance of UV light by the clay in solution, it does so in a linear fashion in relation to concentration, and therefore the concentration of the clay can be calculated using Beer's Law. The slope of the line that is observed in these experiments needs to be taken into account when using sonicated Ca-Mont because the degree of sonication of a solution will change the level of absorbance for solutions of the same concentration.

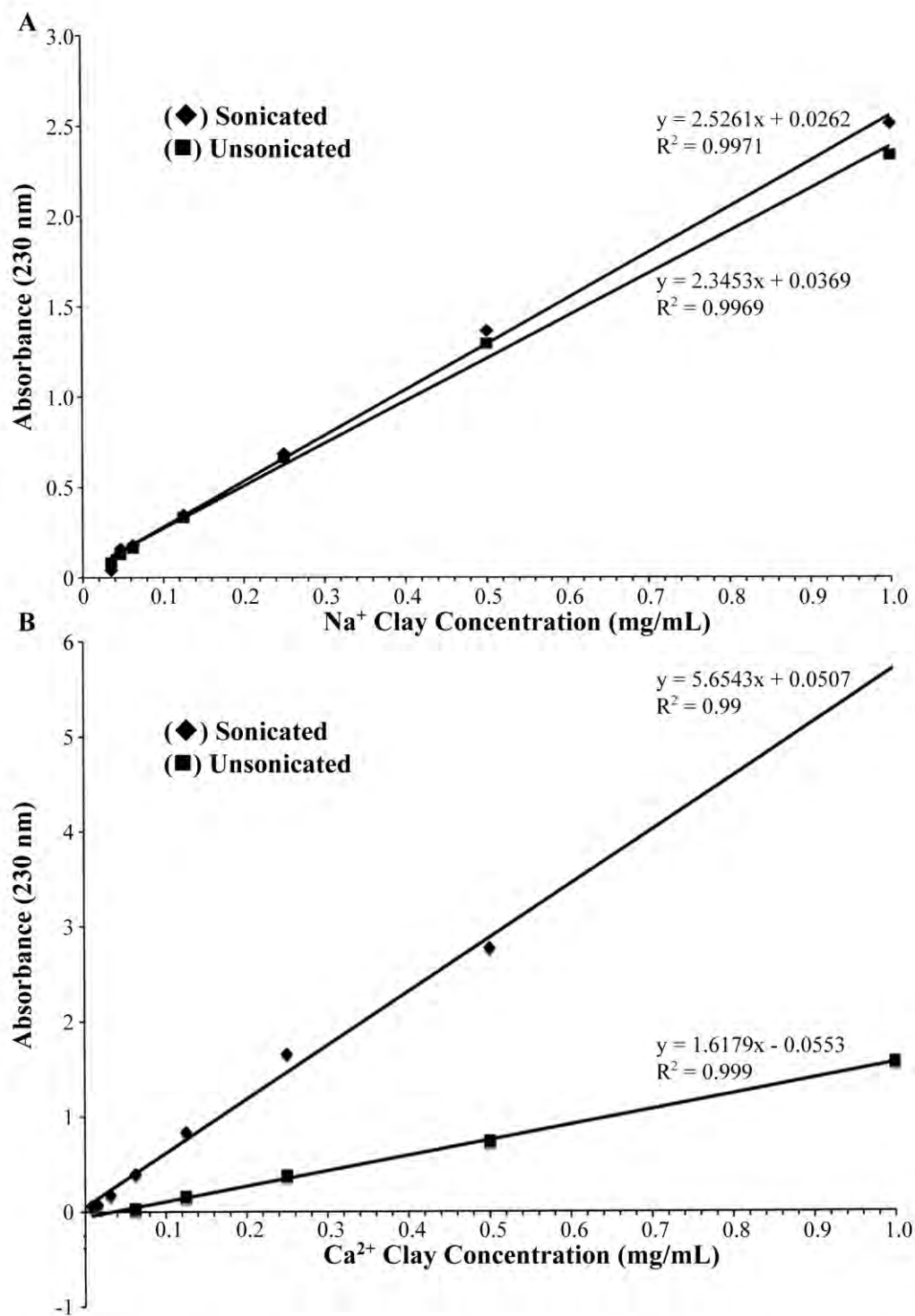


Figure 7. Absorbance of UV light by Montmorillonite. Absorbance at 230 nm by (A) sonicated and unsonicated Na-Mont, and (B) sonicated and unsonicated Ca-Mont demonstrating adherence to Beer's Law.

The experiments shown in Figure 8 involved sonication for 5 min for Na-Mont and 10 min for Ca-Mont. In order to test the effects of varying sonication times, the absorbance of a 0.3 mg/mL solution of Ca-Mont was tested and increased rapidly across 30 sec, 1 min, 2 min, and 3 min (Figure 8). The unsonicated solution had an initial A_{230} of 0.126, which increased to 0.674 at 0.5 min, 0.644 at 1 min, 0.920 at 2 min, and to 1.132 at 3 min. It continued to increase, albeit at lesser pace, at 4 min, 5 min, and with an additional 5 min to the solution that had already been sonicated for 5 min (5 + 5 min). Sonication of the solution for these latter time periods increased the absorbance from 1.009 to 1.277 and then to 1.317. Using the absorbance obtained from the 5 + 5 sonication time trial as the standard for full sonication, the other trials were compared against it as a percentage full sonication. Based on these percentages, we concluded that 3 min of sonication is sufficient to disperse the clay.

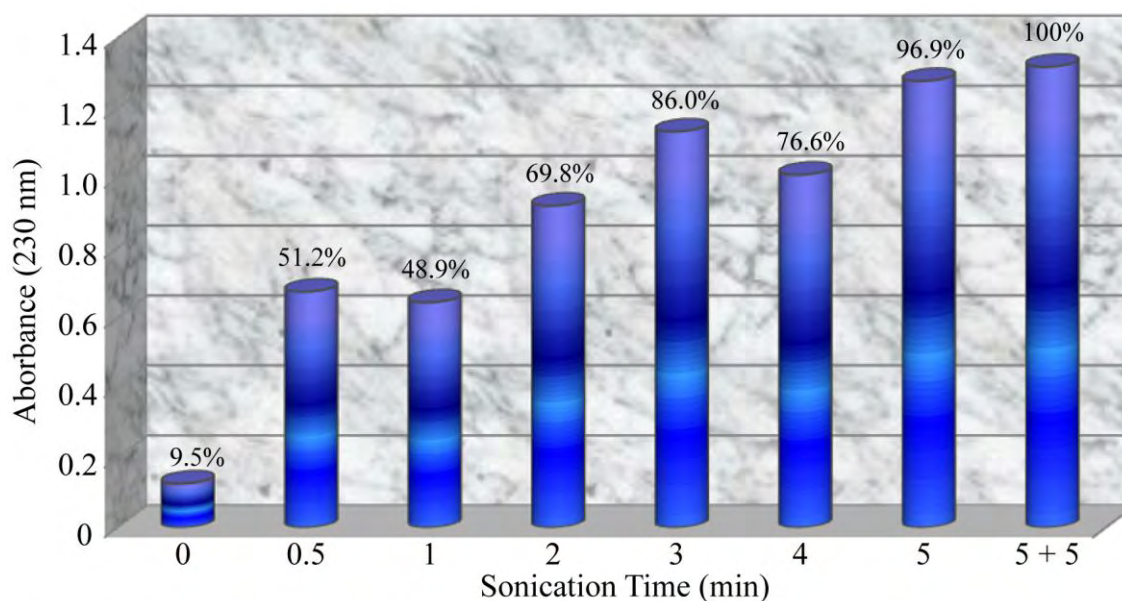


Figure 8. Timed Sonication of Ca-Mont vs Absorbance at 230 nm. The absorbance of the unsonicated Ca-Mont solution was measured from time 0 (no sonication) to an additional 5 min of sonication to the aliquot that had previously been sonicated for 5 min, (5 + 5), for a total of 10 min. Assuming 100% dispersion at 5 + 5, the percentages above each column show dispersion in relation to the 5 + 5 sonication trial.

Platelets of homoionic montmorillonite precipitate inefficiently under conventional centrifugation conditions. Due to the high mass and insolubility of clay particles, in conjunction with the observation that clay sediments rapidly, it has been uncontested that essentially all of the clay in solution sediments with time, especially after centrifugation. Using this logic, researchers concluded that all of the clay would pellet when exposed to centrifugation (3-6, 22-27, 30, 32, 34, 35).

Beer's Law was employed to quantify sedimentation efficiencies of two homoionic clay types. Aliquots of 5 mg/mL Ca-Mont solution and an equally concentrated solution of Na-Mont in ddH₂O were centrifuged at 18,000g and 40,000g. 18,000g was the typical g-force used by previous researchers in clay-DNA binding

studies and 40,000g was the highest g-force used in any of those studies. The supernatant was monitored for absorbance at 230 nm and 260 nm. At 18,000g, the concentration of Na-Mont was reduced from 5.0 mg/mL to 0.85 mg/mL, which leaves almost 20% of the original clay concentration suspended in solution (Table 1).

Table 1. Fractions of Na and Ca Montmorillonite Clays That Are Resistant to Precipitation by High-Speed Centrifugation in Unsonicated Aqueous Solutions

Homoionic Clay	Initial [Clay] (mg/mL)	Centriguge Speed (g)	Supernatant			Predicted [dsDNA] (μ g/mL) ^b
			A ₂₃₀	Final [Clay] (mg/mL) ^a	A ₂₆₀	
Na	5	18,000	2.04	0.85	1.40	70.0
Na	5	40,000	0.34	0.13	0.19	9.5
Ca	5	18,000	0.65	0.11	0.29	14.5
Ca	5	40,000	0.24	0.03	0.13	6.4

^a Residual clay concentrations were calculated on the basis of A₂₃₀ values according to the Beer's law relationships depicted in Figure 2. Samples were centrifuged for 20 min at 18,000 or 40,000g. ^b Predicted concentration of free double-stranded DNA (not bound by clay particles) if employed for clay-DNA binding study. Theoretical DNA concentrations were calculated on the basis of the standard relationship: A₂₆₀ of 1.00 = 50 mg/mL DNA.

Ca-Mont pellets more efficiently, leaving a relatively low concentration of 0.11 mg/mL remaining in the supernatant. Centrifugation at 40,000g improved sedimentation efficiencies, but the resulting supernatants still retained absorbances of 0.19 and 0.13 at 260 nm for the Na-Mont and Ca-Mont clays, respectively.

The resulting absorbances complicate the quantification of free DNA. Using Beer's law to calculate the concentration of DNA by utilizing its absorbance at 260 nm, it is known that absorbance is also linearly proportional to the concentration whereby an

A_{260} of 1.0 corresponds to a concentration of 33 $\mu\text{g/mL}$ of ssDNA oligonucleotides or 50 $\mu\text{g/mL}$ of dsDNA (42). The absorbance of unsedimented residual clay at 260 nm resulted in a substantial overestimation of free DNA in clay-DNA binding assays by previous researchers investigating clay binding to DNA. What they likely did not account for was the presence of small particles of clay that remain dispersed in suspension due to their small size. These clay particles resist pelleting during centrifugation. In order to properly quantify the concentration of unadsorbed DNA, one must take into account the unpelleted clay in the solution. These data would suggest that all previously published assays had a constant error due to this overestimation of free DNA.

An impact study of sonication on clay after centrifugation at 18,000g reveals that sonication causes the precipitation of clay to be even more inefficient (Table 2). Unpelleted clay in the supernatant was shown to be significantly higher for both sonicated Na-Mont and Ca-Mont, with residual Ca-Mont being 10-fold higher than the unsonicated solution after centrifugation at the same speed. The amount of residual absorbance at 260 nm remains high in tandem with the absorbance at 230 nm, thus resulting in flawed measurement of free DNA. This same technique was used by a small number of clay-DNA researchers, who unwittingly exacerbated the problem of unsedimented clay when conducting their assays with sonicated solutions.

Table 2. Impact of Sonication on Sedimentation of Na and Ca Montmorillonite Clays

Homoionic Clay	Initial [Clay] (mg/mL)	Supernatant		
		A_{230}	[Clay] (mg/mL) ^a	A_{260}
Na (Unsonicated)	2	0.61	0.24	0.52
Na (Sonicated)	2	1.46	0.61	1.22
Ca (Unsonicated)	2	0.17	0.02	0.16
Ca (Sonicated)	2	1.60	0.27	1.36

^a Residual clay concentrations were calculated using the equations derived in Figure 7. Sonicated or unsonicated clay suspensions were centrifuged for 20 min at 18,000g.

An assessment of the ability of heat to separate clay platelets. Dispersion of clay platelets in solution may be affected by several factors. A different approach to separate the tactoids is by heat. Electrostatic forces can be overcome by the input of energy in much the same way that a substance will change states from solid to liquid and then to gas as heat energy enters the system, or as is common to biochemistry, the separation of double-stranded DNA into single strands. To measure the dispersion of clay, we measured the absorbance of two disparate wavelengths of UV light in a diluted clay solution, 230 nm and 450 nm. The 230 nm wavelength was selected once again because that is the maxima of UV light absorption of clay. The second wavelength measured, 450 nm, was chosen because it resides in the area of the spectrum where any apparent absorbance would be caused by light scattering instead of true absorbance. In this region of the spectrum, the absorbance of the solution remains low and constant. If the majority of the platelets have aggregated into tactoids in a dilute solution, they would allow much of the UV light to pass through the sample solvent and be detected. As the

level of dispersion increases and the tactoids become separated into individual platelets, more of the UV light would be absorbed due to the more complete accessibility of the platelets within the solution. As heat energy is added, the amount of dispersion into individual platelets should increase over time. Due to the observed increase in absorbance caused by sonication of Ca-Mont (Figure 7), this clay was used for all experiments involving heating clay solutions. A 0.3 mg/mL solution of unsonicated Ca-Mont, which forms large tactoids and rapidly sediments, showed an initial A_{230} of 0.242 and an initial A_{450} of 0.123 (Figure 9). As the heating continued, the absorbance at these two wavelengths increased in a somewhat linear trend across 3 min, 5 min, 10 min, 20 min, and 30 min until the absorbance levels ultimately doubled.

Heated clays did not achieve the same magnitude of absorption at 230 nm as they did for sonication. The control sample of Ca-Mont that was subjected to 5 min of sonication absorbed UV light about 5 times more than heated solutions of the same clay. As Figure 9 demonstrates, the 230 nm absorption of the control was around 2.000 compared to around 0.400, which was the highest level of absorbance observed by heating. By contrast, due to the nature of what causes absorbance in clay, which is the levels of accessible Fe (III), the higher level of absorbance at 230 nm seen with sonication may be more desirable because it suggests a more thorough dissociation of the platelets. The increase in absorbance is indicative of the increased dispersion of the clay. However, since the increase is much more drastic than heating alone, this suggests that more may be happening than simple dispersion. It is possible that sonication is breaking covalent bonds in the platelets and exposing more Fe (II) that becomes oxidized to Fe

(III) or altering the bonding structure of the lattice in such a way that absorbance is increased.

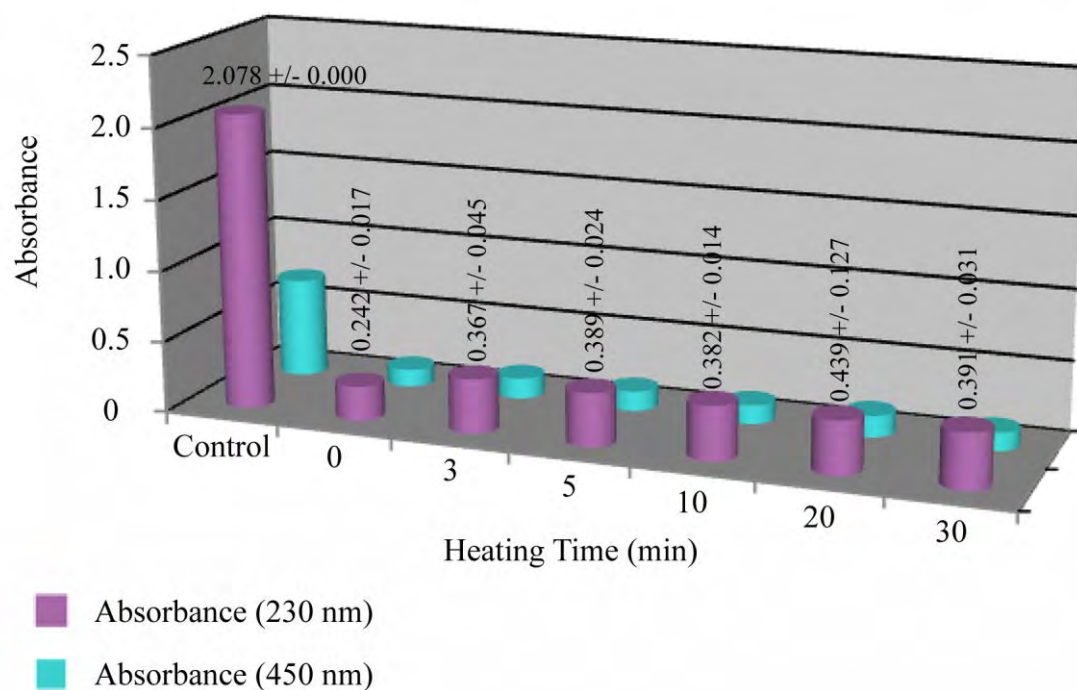


Figure 9. Plot of 100 °C Heating Times vs Absorbance at 230 nm and 450 nm. The absorbance of the unsonicated Ca-Mont solution was measured from time 0 (no heat) to 30 min of 100 °C heat, and compared against the control, which was an aliquot of the same stock solution that had been sonicated for 5 min. The numbers above each column are the average absorbance at 230 nm with standard deviation for each trial, which was performed in quadruplicate.

Additional comparative studies were conducted to see how heating a clay solution disperses clay in relation to sonication, which is the standard method employed by clay scientists. To do this, an $A_{230}:A_{450}$ ratio was established by which a number would indicate the degree of dispersion whereby the higher the number, the more dispersed the clay. Due to the dramatic increase in absorbance at 230 nm and the relatively stable levels

of absorbance at 450 nm, the ratio should indicate the level of uniformity of the dispersion of clay platelets. We measured the absorbance of the clay over time at 30 sec, 1 min, 2 min, 3 min, 4 min, 5 min, and 10 min after sonication as described in Materials & Methods and calculated this ratio to gauge dispersion (Figure 10). The $A_{230}:A_{450}$ ratio increased steadily to 3.0 at 3 min and remained at about that level through 5 min. At 10 min the $A_{230}:A_{450}$ ratio reached 3.3, but results suggest that 3 min is an indication of maximum dispersal by sonication. Interestingly, heating at 100 °C caused the $A_{230}:A_{450}$ ratio to increase to approximately 3.0 as well. At present it is unclear why heating and sonication produced identical results for the wavelength ratios, but not for the individual wavelength analysis at 230 nm.

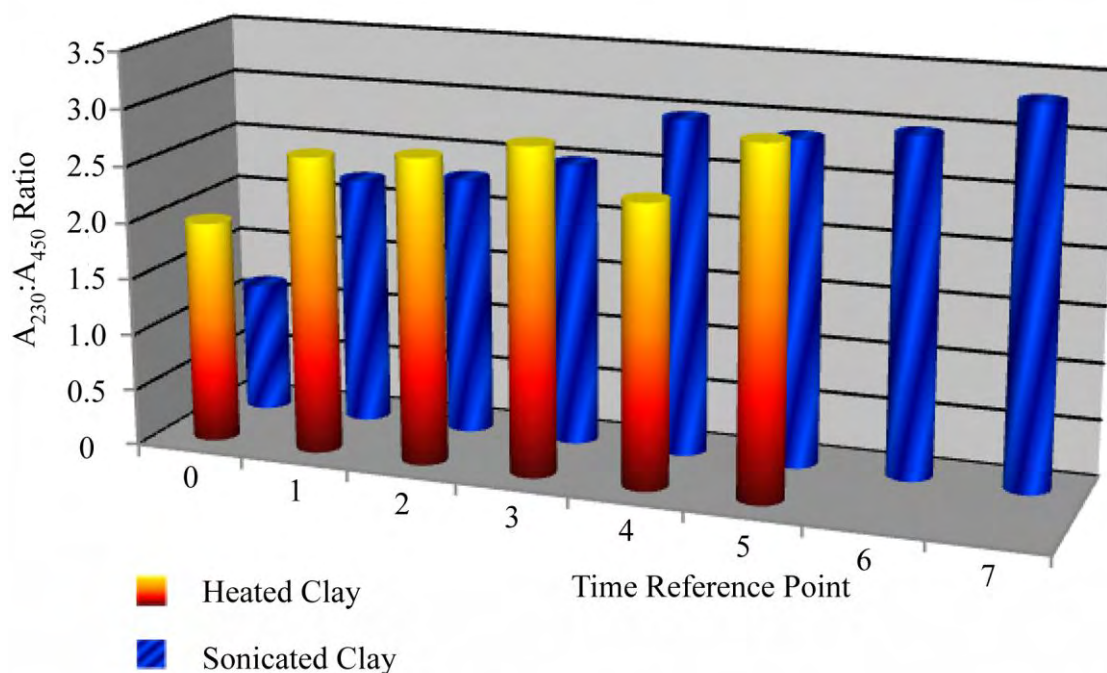


Figure 10. Comparison of $A_{230}:A_{450}$ Ratios. Ca-Mont that has been heated or sonicated for various times. For heated clay, 0, 3, 5, 10, 20, and 30 min correspond to time reference points 0 - 5, respectively. For the sonicated clay set, 0, 0.5, 1, 2, 3, 4, 5, and 5 + 5 min correspond to time reference points 0 - 7 respectively.

Filtration can be employed to remove most clay particles from a solution. In an attempt to alleviate the contribution to absorbance by residual clay in a solution, filtration techniques were tested as an alternative to centrifugation. Solutions of both sonicated and unsonicated 2 mg/mL Na-Mont were passed through a 0.2 μm Nalgene filter apparatus by aspiration or through a 0.2 μm Millex disc filter with the assistance of a 5 mL syringe. Absorbance was measured at 230 nm before and after filtration (Table 3). Filtration of unsonicated Na-Mont reduced the amount of clay in the solution by 85.5% with the Nalgene filter and 88.9% with the Millex filter. To test the effects of a second filtration, an unsonicated Na-Mont solution was passed through the Millex filter and measured for absorbance at 230 nm. The filtrate was then passed once again through a Millex filter and measured for absorbance at the same wavelength. After the first filtration, 11.2% of the original clay remained in the solution. After the second filtration, 9.6% of the clay was still in suspension. Sonicated clay yielded similar results, with 13.0% remaining after the first filtration and a similar amount, 16.0% after the second.

Table 3. Analysis of Residual Clay After Filtration of Na Montmorillonite

A	Nalgene Filter (0.2 μm)	Millex Filter (0.2 μm)
Unsonicated Na-Mont	14.5%	11.1%
Sonicated Na-Mont	46.5%	8.5%

B	1st Filtration	2nd Filtration
Unsonicated Na-Mont	11.2%	9.6%
Sonicated Na-Mont	13.0%	16.0%

Filtration of Na-Mont. (A) Nalgene 0.2 μm aspirated filter and the Millex 0.2 μm disc filter attached to a 5 mL syringe were used to reduce the A_{230} of a sonicated and an unsonicated Na-Mont solution. (B) The Millex 0.2 μm disc filter was used to filter a sonicated and an unsonicated Na-Mont solution twice, and the percentage of the absorbance at 230 nm that remained in the filtrate was measured.

Employing filtration methods appears to be effective in separating large platelets from smaller ones. A 0.2 μm filter is capable of removing 90% of the clay from a solution, which is as efficient as centrifugation at speeds that are normally used. This suggests that filtration may be a useful alternative to centrifugation in clay-DNA binding studies as long as the DNA does not adhere to the filter membrane. It also indicates that the larger components of a clay solution can be separated from the small components, and therefore a protocol for future clay-DNA binding experiments using only large platelet clay may be developed.

The addition of salt aids in the precipitation of clay from solution. The effects of altering concentrations of salts such as NaCl or MgCl_2 on the affinity of DNA for clay surfaces has been investigated using centrifugation methods, but the effect on the precipitation of the clay particles was heretofore not completely characterized. We

investigated the possibility that salt concentration may affect the sedimentation of clay platelets differently. Absorbance of sonicated solutions of 0.5 mg/mL Na-Mont and Ca-Mont were measured at 230 nm before and after centrifugation in the presence of varying concentrations of NaCl or MgCl₂ (Figure 11). While salt did not affect the sedimentation of uncentrifuged clay, a concentration-dependent relationship was observed on the pelleting of clay particles by centrifugation. NaCl at concentrations of 10 mM and lower showed little effect on precipitation, but concentrations of 100 mM showed a decrease in supernatant absorbance at 230 nm, indicating an increase in sedimentation efficiency. By contrast, the addition of MgCl₂ produced more efficient pelleting at lower concentrations of the salt. A comparatively low concentration of 1 mM MgCl₂ was enough to strongly enhance the precipitation of both types of clay after centrifugation (dark gray bars in Figure 11).

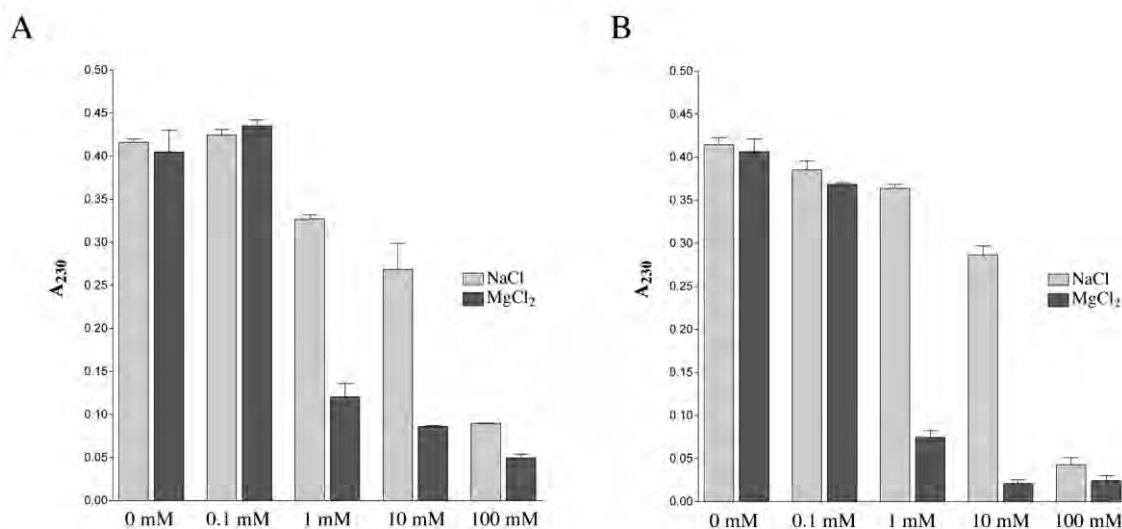


Figure 11. Effect of Salt on the Sedimentation Efficiencies of (A) Na Montmorillonite and (B) Ca Montmorillonite. Absorbance at 230 nm was monitored after centrifugation of clay suspensions for 15 min at 18,000g. Error bars indicate standard deviations.

Montmorillonite platelets come in a variety of sizes, being around 1 nm thick and the smallest being about 20 nm in the lateral dimensions and the largest approaching 1,000 nm in the same two dimensions. Assuming an average sheet size of 1 x 200 x 200 nm³, the molecular weight of clay is approximately 4.44×10^7 . This was calculated on the basis of a regular 2:1 layered structure of clay and assuming negligible contribution from water and Na or Ca ions associated with the dry powder clay at 2 to 4%. As previously cited, the 0.5 mg/mL clay solutions exhibited a threshold effect where a transition from 10 to 100 mM NaCl greatly increased the efficiency of precipitation. This means that a critical contribution of positive charges from Na⁺ is achieved in transition from a Na-to-clay molar ratio of 900,000 to 9,000,000 ions per platelet, whereby aggregation of the platelets facilitated precipitation. This same threshold was observed when the Mg-to-clay

molar ratio increased from 9,000 to 90,000 ions per platelet. The logical conclusion is that the increased sensitivity of clay to magnesium is the result of the greater charge density of Mg^{2+} over Na^+ , which improves its ability to promote aggregation of platelets into tactoids.

A new assay for the adsorption of DNA to clay particles reduces problems associated with overestimation of unbound DNA. If the absorption contribution of unsedimented montmorillonite clay at 260 nm is taken into account, even after high-speed centrifugation, it is possible to design an improved clay-DNA binding assay from the method employed in previous studies (3-6, 22-27, 30, 32, 34, 35). Sonicated Na-Mont was used to bind the ssDNA oligonucleotide Pvu4a, a 25-mer, and the new assay was employed to quantitate the amount of unbound DNA (Table 4). The experiments involved a simultaneous control experiment where 0.5 mg/mL clay and a mixture of 0.5 mg/mL clay and 20 $\mu\text{g/mL}$ of DNA were separately centrifuged at 18,000g for 15 min. For each solution, the supernatant was analyzed for absorbance at 260 nm. The resulting A_{260} from the supernatant of the clay only solution was subtracted from that of the clay + DNA solution, which resulted in a corrected calculation of free DNA. These experiments were performed in triplicate or quadruplicate, and with or without the mono- or divalent cations from NaCl or MgCl_2 .

Addition of NaCl had no observed effect on the association of oligonucleotide DNA with Na-Mont clay particles at concentrations ranging from 0.1 mM to 100 mM (Table 4). In the presence of the monovalent cation at these concentrations, the amount of bound DNA stagnated between 22 and 30%. The results indicate that the interaction

between the DNA and the exchangeable cations on the surface is not strong due to a limited amount of exchange sites. The dilute concentration of Na ion concentration in solution would not be expected to change the sorption of the DNA. The clay-DNA interaction with 0.1 mM MgCl_2 was similar to that of the NaCl, with the clay only able to bind 26% of the DNA present in the solution. However, binding was greatly enhanced at higher concentrations of magnesium. Experiments using the same incremental increases in salt concentration were tested, and from 1.0 mM to 100 mM MgCl_2 , the fraction of DNA that had successfully bound to clay leapt to 85, 92, and 91% for each successive increment. On a brief aside, it is important to note that Pvu4a does not precipitate under the aforementioned conditions. As a control to test for the precipitation of DNA by association with cations along the molecule, solutions of DNA and salt in the predetermined concentrations were also analyzed post-centrifugation for A_{260} . Even solutions containing the highest concentrations of salt (100 mM) showed no reduction of DNA in solution.

The experiments presented in Table 4 were repeated with the exception of sonicated Ca-Mont taking the place of the Na-Mont. Addition of NaCl increased binding of DNA to the Ca-Mont clay only moderately, reaching 46% and 58% bound at 10 mM and 100 mM NaCl, respectively (Table 5). In contrast, addition of 0.1 mM MgCl_2 increased DNA binding up to 73% and up to 93%, 95%, and 94% at 1 mM, 10 mM, and 100 mM MgCl_2 . Results with both of the clays and the salts NaCl and MgCl_2 are summarized in Figure 12. All of these results are consistent and they demonstrate that binding of DNA to clay is strongly dependent upon the type of ions that are present.

Table 4. Impact of Na and Mg Counterions on Binding of Single-Stranded Oligonucleotide DNA to Sonicated Homoionic Na Montmorillonite^a

Assay Components			([Clay + DNA] Free				
NaCl (mM)	Clay	DNA	Supernatant A_{260}	-[Clay] ΔA_{260}	[DNA] ($\mu\text{g/mL}$)	Bound [DNA]	% DNA _i Bound
0	-	+	0.685	N/A	22.6	N/A	N/A
0	+	-	0.354				
0	+	+	0.842	0.488	16.1	6.5	29
0.1	+	-	0.315				
0.1	+	+	0.853	0.538	17.8	4.8	22
1.0	+	-	0.330				
1.0	+	+	0.837	0.507	16.7	5.9	26
10	+	-	0.339				
10	+	+	0.818	0.479	15.8	6.8	30
100	+	-	0.263				
100	+	+	0.739	0.476	15.7	6.9	30
MgCl ₂ (mM)							
0	-	+	0.685	N/A	22.6	N/A	N/A
0	+	-	0.359				
0	+	+	0.878	0.519	17.0	5.0	22
0.1	+	-	0.344				
0.1	+	+	0.847	0.503	16.6	6.0	26
1.0	+	-	0.302				
1.0	+	+	0.409	0.107	3.5	19.1	85
10	+	-	0.283				
10	+	+	0.338	0.055	1.8	20.8	92
100	+	-	0.241				
100	+	+	0.300	0.059	1.9	20.6	91

^a Clay suspensions with or without added NaCl or MgCl₂ were centrifuged for 15 min at 18,000g. Bound DNA = initial DNA concentration ([DNA]_i) - free [DNA] expressed as $\mu\text{g/mL}$. N/A: Not applicable.

Table 5. Impact of Na and Mg Counterions on Binding of Single-Stranded Oligonucleotide DNA to Sonicated Homoionic Ca Montmorillonite^a

Assay Components			([Clay + DNA] - [Clay])		Free [DNA]	Bound [DNA]	% DNA _i Bound
NaCl (mM)	Clay	DNA	Supernatant A ₂₆₀	ΔA ₂₆₀	(μg/mL)		
0	-	+	0.813	N/A	26.8	N/A	N/A
0	+	-	0.536				
0	+	+	1.088	0.552	18.2	8.6	32
0.1	+	-	0.590				
0.1	+	+	1.098	0.508	16.7	10.1	38
1.0	+	-	0.843				
1.0	+	+	1.247	0.404	13.3	13.5	50
10	+	-	0.762				
10	+	+	1.201	0.440	14.5	12.3	46
100	+	-	0.659				
100	+	+	0.996	0.337	11.1	15.7	58
MgCl ₂ (mM)							
0	-	+	0.791	N/A	26.1	N/A	N/A
0	+	-	0.494				
0	+	+	0.931	0.437	14.4	11.7	45
0.1	+	-	0.563				
0.1	+	+	0.778	0.215	7.1	19.0	73
1.0	+	-	0.447				
1.0	+	+	0.499	0.052	1.7	24.4	93
10	+	-	0.441				
10	+	+	0.482	0.041	1.4	24.7	95
100	+	-	0.395				
100	+	+	0.440	0.046	1.5	24.6	94

^a Clay suspensions with or without added NaCl or MgCl₂ were centrifuged for 15 min at 18,000g. Bound DNA = initial DNA concentration ([DNA]_i) - free [DNA] expressed as μg/mL. N/A: Not applicable.

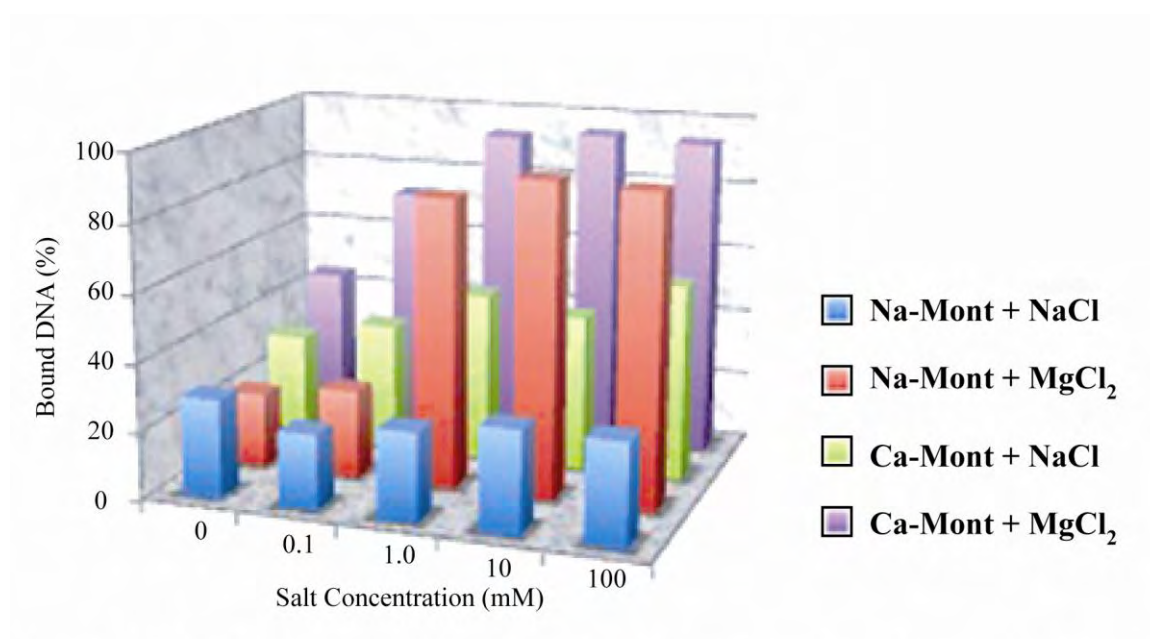


Figure 12. Plot of percentage of DNA bound to clay vs. increasing salt concentration. Sonicated Na clay and Ca clay was used for all experiments.

To contrast the new approach with the assay method used in past studies, the experiments were repeated using the old technique and the results compared (Figure 13). For the old assay, MgCl₂ and unsonicated clays were used and the absorbance of the unsedimented clay was not accounted for in the samples. The fractions of DNA bound to unsonicated Na-Mont and Ca-Mont in the presence of increasing concentrations of MgCl₂ were compared against fractions bound using the new assay. Both Na-Mont and Ca-Mont in the old assay exhibited a smaller fraction bound due to overestimation of free DNA resulting from clay remaining in the supernatant after centrifugation.

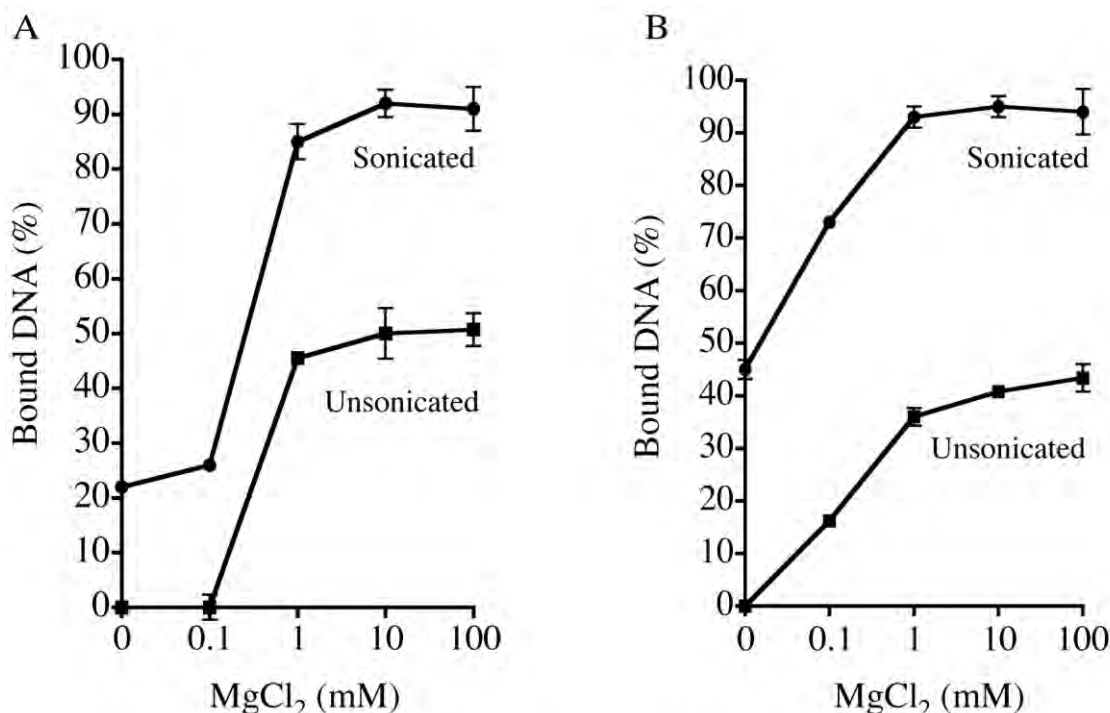


Figure 13. New Binding Assay Method vs Previous Binding Assay Method. Comparison of DNA adsorbed onto (A) Na montmorillonite and (B) Ca montmorillonite with or without MgCl₂. Experiments utilized previously described methods with unsonicated clay (■) or the new protocol employing sonicated clay and subtraction of A₂₆₀ contributions due to unsedimented clay (●).

Clay will efficiently adsorb dsDNA in solution. Similar experiments to the ssDNA-clay binding experiments were conducted using a double-stranded DNA 25-mer (Pvu4a + cPvu4a) with either Na-Mont or Ca-Mont and increasing concentrations of NaCl or MgCl₂. The new, improved assay was used to quantify bound DNA. The double-stranded Pvu4a-cPvu4a complex was made by combining the two types of oligomer in equal concentrations in ddH₂O with or without added salt. The solution was heated to 95 °C and cooled slowly to RT. To verify the annealing of the strands into a dsDNA complex, the products were analyzed by electrophoresis on a 4% agarose gel and their migration compared against those of the single-stranded oligonucleotides and DNA

molecular weight standards (Figure 14). Ethidium bromide was used to stain the DNA, which fluoresces in the presence of UV light. Lanes 2 and 3, which contained the single-stranded oligomers, both showed small, faint bands. This was to be expected, as ethidium bromide is not very effective at staining ssDNA. However, a larger, more intensely stained band was observed in lanes 4 – 6, which indicates that the 2 complementary strands annealed to form a double-stranded complex. Although the bands are somewhat diffuse, annealing in water, 10 mM NaCl, and 10 mM MgCl₂ all generated a larger band corresponding to dsDNA. The strongest band was seen in lane 6, where the two oligomers were combined in the presence of 1 mM MgCl₂, suggesting that the added salt enhanced the annealing of the complementary strands, though it is possible that the salt simply enhanced staining. Further confirmation of the annealing of the complements is seen in the position of the bands. The bands in lanes 2 and 3 are positioned further down the gel than in lanes 4 – 6 due to the smaller size of the ssDNA molecules than their dsDNA counterparts in the last three lanes.

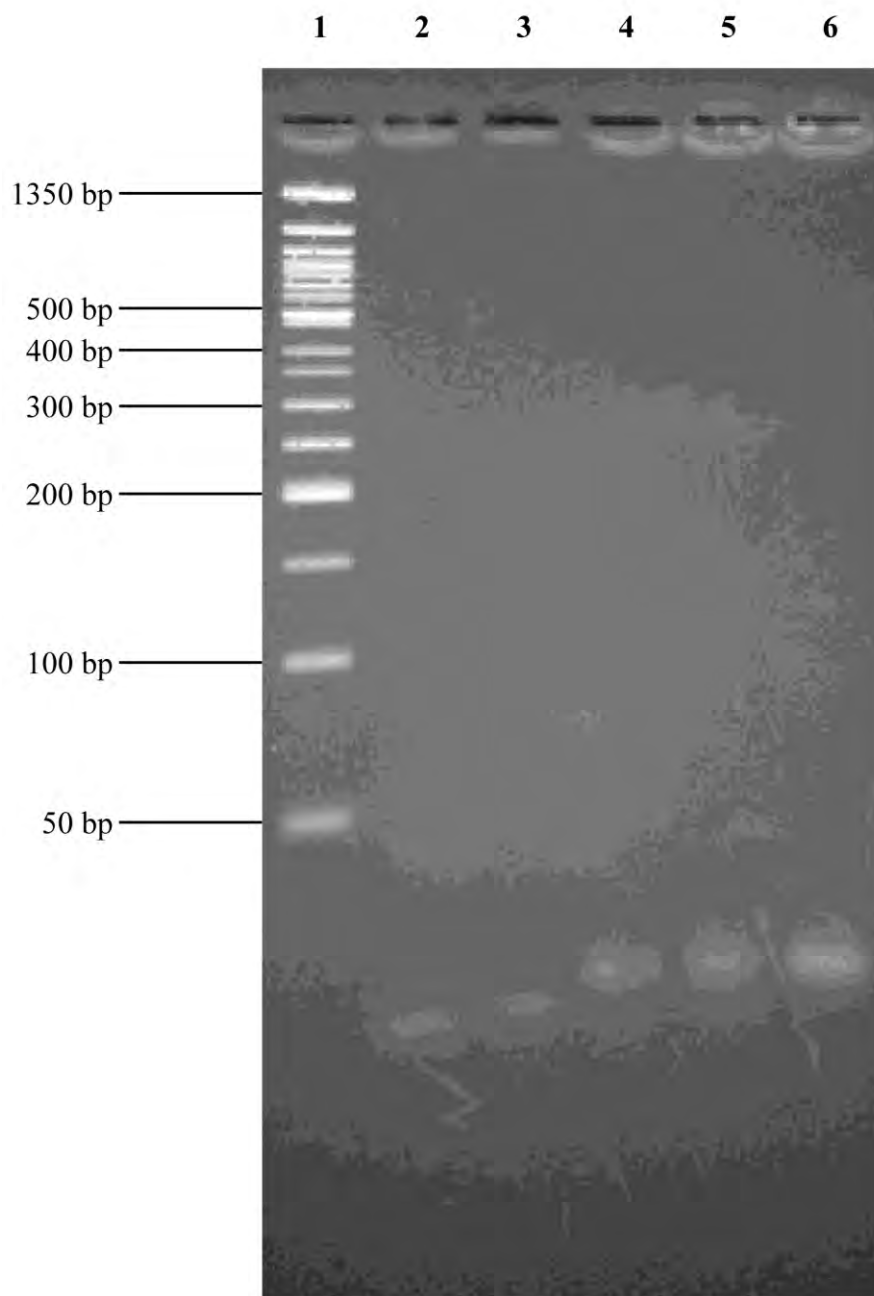


Figure 14. Agarose Gel with Single and Double Stranded 25-mer DNA. Agarose gel (4%) illustrating the DNA complex. (1) 50 base pair DNA ladder standard, (2) ssDNA Pvu4a 25-mer, (3) ssDNA cPvu4a 25-mer, (4) Pvu4a + cPvu4a, (5) Pvu4a + cPvu4a + 10 mM NaCl, (6) Pvu4a + cPvu4a + 10 mM $MgCl_2$.

Interestingly, mixing dsDNA with sonicated Na-Mont produced a binding efficiency of 85.0% in the absence of added NaCl, which is strikingly different from the observed data from the clay-ssDNA binding experiments and may be an indication that the higher negative charge density of the dsDNA results in a higher affinity for the clay. NaCl was incrementally increased from 0.1 to 100 mM and bound fractions increased modestly to 86.5%, 91.0%, 88.0%, and eventually to 92.4% under high salt conditions. This trend once again demonstrates that the addition of NaCl does not have a strong effect on binding of DNA, as was seen previously for ssDNA.

In the same fashion, 80.1% of the dsDNA bound to sonicated Na-Mont without cation enrichment by additional MgCl_2 . In the presence of 0.1 mM MgCl_2 binding was similar at 75.6%. When the concentration of MgCl_2 was increased to 1 mM, 94.9% of the DNA was bound to the clay. The percentage bound leveled off from this point on at higher concentrations, moving to 97.2% in 10 mM MgCl_2 and 94.3% bound in 100 mM MgCl_2 .

The binding of dsDNA to sonicated Ca-Mont was investigated as well, though only two measurements were made for each concentration of salt in these experiments. In this experiment, with no additional salt added to the solution, sonicated Ca-Mont bound 82.7% of the DNA. The percent bound remained stable at 81.3% when the NaCl of the solution was increased to 0.1 mM. As more salt was added, the percent bound increased to 94.1% with 1 mM NaCl, 87.5% with 10 mM NaCl, and 91.6% with 100 mM NaCl.

When MgCl_2 was added to a solution containing dsDNA and sonicated Ca-Mont, the same pattern emerged where binding started high and increased to near full

efficiency. In a clay solution without salt, we found that 73.9% of the DNA was bound upon centrifugation. When the salt concentration was increased to 0.1 mM MgCl_2 , 86.8% of the DNA adsorbed. As the molarity was increased from 1 mM to 10 mM to 100 mM MgCl_2 , binding efficiency was nearly maximal at 100.0%, 100%, and 99.0%, respectively.

It is worth repeating here that the experiments using sonicated Ca-Mont were only conducted twice in quadruplicate trials using NaCl, and one time in quadruplicate with MgCl_2 added to the solution, and therefore the reproducibility of our results has not been confirmed. That being said, our results do follow previously observed trends and we can state, with some degree of certainty, that the results will be able to be replicated. Due to the strong binding of dsDNA to clay without the addition of a cation, the increase in binding that is observed as the molarity of salt is raised is not nearly as illustrative as desired. Future experiments will confirm or deny this, but it is our contention that they should be conducted using a lower concentration of clay so that we can better gauge the degree to which an increase in salt will affect adsorption.

Adsorption of ssDNA onto sonicated montmorillonite produces intercalated structures. In order to properly investigate clay-DNA binding, it is important to understand how this occurs. As mentioned in Chapter I, it is possible that the DNA adsorbs to the exterior of clay tactoids, intercalates within the tactoids, or binds to the individual platelets as they sediment in a random fashion instead of the tactoidal conformation. Cerius 2 molecular modeling software has been used to predict the gallery spacing in polymer-clay nanocomposites by Dr. Beall (43). The same approach was used

to analyze and predict clay-DNA structures. Lowest energy structures were predicted for each of the two clays with the oligonucleotide ssDNA (Figure 15) (44). The modeling predicted that the clay plates form bridges between the negative phosphate groups of the DNA using the cations in the space between the two surfaces. The computer model predicted a d spacing, the gallery size between the platelets, of 2.04 nm for Na-Mont and 1.84 nm for Ca-Mont.

Structural analysis of the complexes formed by the binding of ssDNA oligonucleotide Pvu4a to the sonicated clay in the presence of 10 mM MgCl_2 was performed using X-ray diffractometry. Samples were prepared by combining the clay, DNA, and salt in a 40 mL Oak Ridge tube and centrifuging at high g force. The pellet was then smeared on a glass slide. A high clay to DNA ratio of 2:1 was used to increase the likelihood that the intercalation would be detected. The d spacing of the galleries was measured to be 2.06 and 1.88 nm for Na-Mont and Ca-Mont, respectively. The actual measurement deviated from the predicted spacing by 1.5 and 2.1%, again respectively. The spacing is increased by 1.06 and 0.88 nm over that of the interplatelet spacing of dehydrated Na-Mont and Ca-Mont, which is evidence that the gallery has been expanded by the width of ssDNA, which has a diameter of about 1 nm.

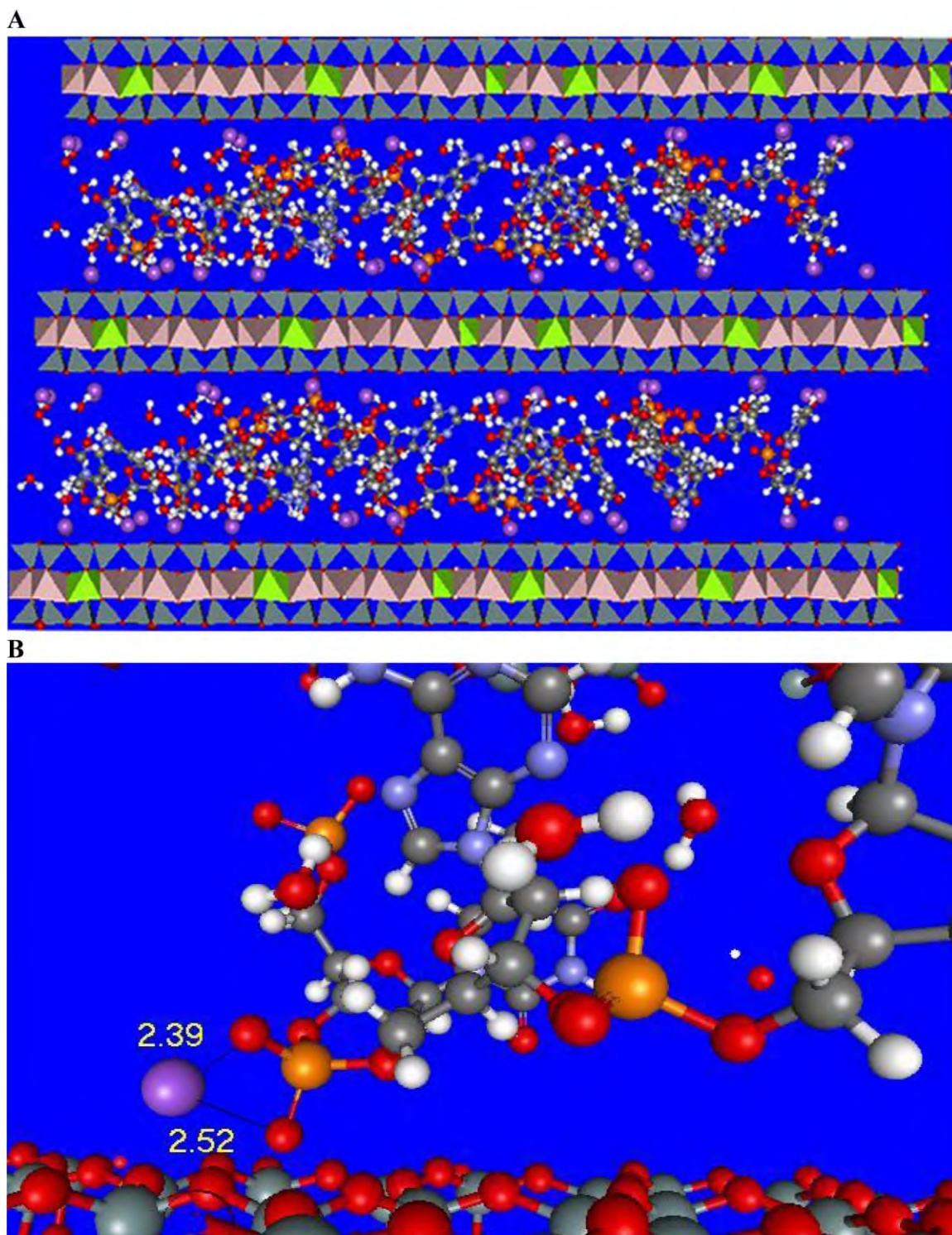


Figure 15. Computer Model of ssDNA Intercalated Within a Na Montmorillonite Tactoid. (A) Atomic structure of Na montmorillonite platelets associated with intercalated single-stranded DNA predicted by Cerius 2 molecular modeling program after energy minimization iterations. Purple, red, white, gray, orange, and silver spheres correspond to sodium, oxygen, hydrogen, carbon, phosphorus, and silicon ions, respectively. (B) Detailed view of cation bridging interactions with bond distances between a representative sodium atom and two oxygen atoms shown (given by the program in angstroms).

The structures that are formed by the binding of double-stranded DNA to clay were also investigated using X-ray diffraction, but the results were inconclusive. Our results suggested that the DNA did in fact intercalate, but was perhaps broken into single strands due to the spacing of the galleries, which coincided with the single-stranded DNA intercalation observed in the previous experiment (45) Additional experiments will need to be performed to understand these structures.

Heating and other induced stresses have an effect on how solutions contained within microfuge tubes absorb UV light. Experimentation into the dispersal of clay platelets in solution led to an interesting observation with ramifications extending well beyond clay studies and into the laboratories of most biochemists. The heating of clay suspensions described earlier was done in standard 1.5 mL microfuge tubes because all of the experiment could be conducted using the same vessel, from heating, to cooling, to centrifugation. Only the measurement of the A_{230} and A_{260} , which were done using cuvettes, did not require a microfuge tube.

In one of the heating experiments, 0.25 mg/mL clay solutions were heated at 100 °C for 30 min, cooled to room temperature, and scanned from 200 nm to 350 nm. Surprisingly, the peak patterns in these dilute clay suspensions changed from the normal clay patterns seen in Figure 7B and 7C. Although clay suspensions normally exhibit maximum absorbance at around 230 nm, the heated solutions displayed the highest absorbance at 260 nm (Figure 16). The results suggested that heating caused a change in the clay that produced a new peak at around 260 nm or that some other phenomenon was involved.

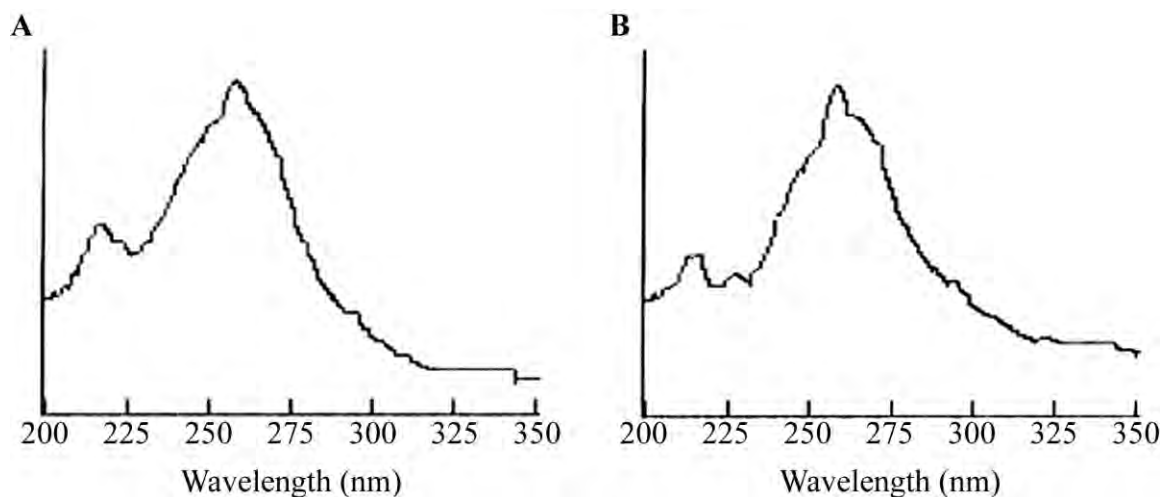


Figure 16. Absorbance Scans of Heated Na and Ca Montmorillonite. Solutions of (A) uncentrifuged, unsonicated Na-Mont, and (B) uncentrifuged, unsonicated Ca-Mont were heated for 30 min at 100 °C and cooled for 2 min in an ice bath. Ambion 12400 tubes were used for this experiment.

The results of the previous experiment led to the question, what was the cause of the new peak observed in the scans? In order to test whether the presence of the clay was required, we heated pure ddH₂O in the tubes, keeping a tube at RT for control, and scanned the solutions (Figure 17). The unheated control showed only noise in the scans and absorbance remained near the baseline of 0.01 – 0.05 across all wavelengths of light. After heating the tube for 30 min at 100 °C and cooling on ice for 2 min (which became the standard protocol for tube heating and will henceforth be assumed), an intense, distinct signature was revealed. A strong, new peak appeared at around 260 nm, which reached 1.100 absorbance units. This peak was similar to the peak observed in the heated clay solutions from Figure 16.

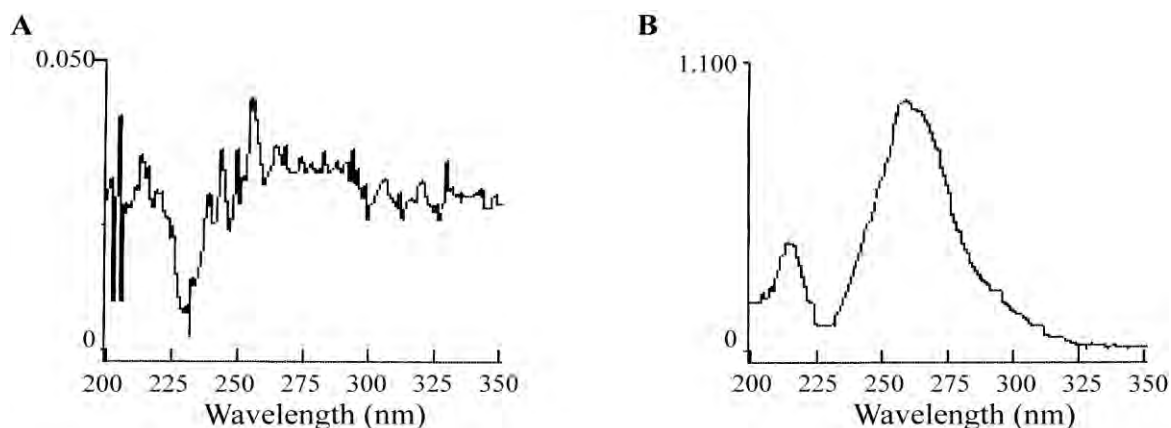


Figure 17. Absorbance Scans of ddH₂O Before and After Heating in a Microfuge Tube. The control (A), which is ddiH₂O taken from a bottle at room temperature, and (B) ddH₂O that was heated for 30 min at 100 °C, and then cooled in an ice bath for 2 min in an Ambion 12400 microfuge tube.

An Internet investigation as to the identity of the chemical that was released into the water upon heating yielded almost no results. The manufacturers of the tubes were reluctant to divulge, or even did not know, the composition of the tubes with the exception of their being comprised of polypropylene plastic. The problem is compounded by the manufacturing process of the tubes, whereby a vender of the tubes will either make them in house or outsource their production. However, the source of the raw polypropylene pellets is not always consistent, and a tube may have polypropylene sourced from several suppliers of raw material. Furthermore, a tube from one batch will have a different percent composition of polypropylene from one supplier than the next batch will due to constant addition of raw polypropylene to the molten stock from which the tubes are made.

Polypropylene plastic microfuge tubes leach chromophoric chemicals. In order to uncover what the chemical is, we first decided to see if this was a universal

problem with microfuge tubes, or if it was a phenomenon isolated to the specific tube type that we were using in the lab. The tube used in all previous experiments was purchased from Ambion (catalogue # AM 12400). A scan of the complete spectrum of UV light (200 nm to 800 nm) of ddH₂O after heating the Ambion tube at 100 °C revealed that all of the absorbance from the leached chemical occurred between 200 nm and 300 nm (Figure 18A). Another brand of tube (VWR catalogue # 20170-038) also leached chemicals and therefore this was not isolated to the Ambion tubes (Figure 18B). The VWR tubes exhibited a high peak at around 220 nm and a smaller peak at about 260 nm, therefore both tubes have peaks near 220 nm and 260 nm, but their relative sizes are reversed. In an attempt to measure the scope of this problem, we tested polypropylene tubes in a variety of sizes from several manufacturers. We found that all of the tubes exhibited leaching, although some had higher UV absorbance from chemicals leached into the water than others. Most brands exhibited a pattern similar to the VWR tubes (Figure 18B) with maximum absorbance near 220 nm. This became the default microfuge tube for all subsequent experiments. The VWR tube did show a different peak pattern than the Ambion tube did, but with peaks at the same wavelengths. The VWR tube typically showed a strong peak at 218 nm and a lesser peak at 258 nm. Due to the universal nature of this problem, we wanted to know if different batches of the same tube model had similar patterns. Scans of multiple batches of a particular brand showed strong consistency throughout, where all of the scans had relatively the same intensity at the same points across the UV spectrum.

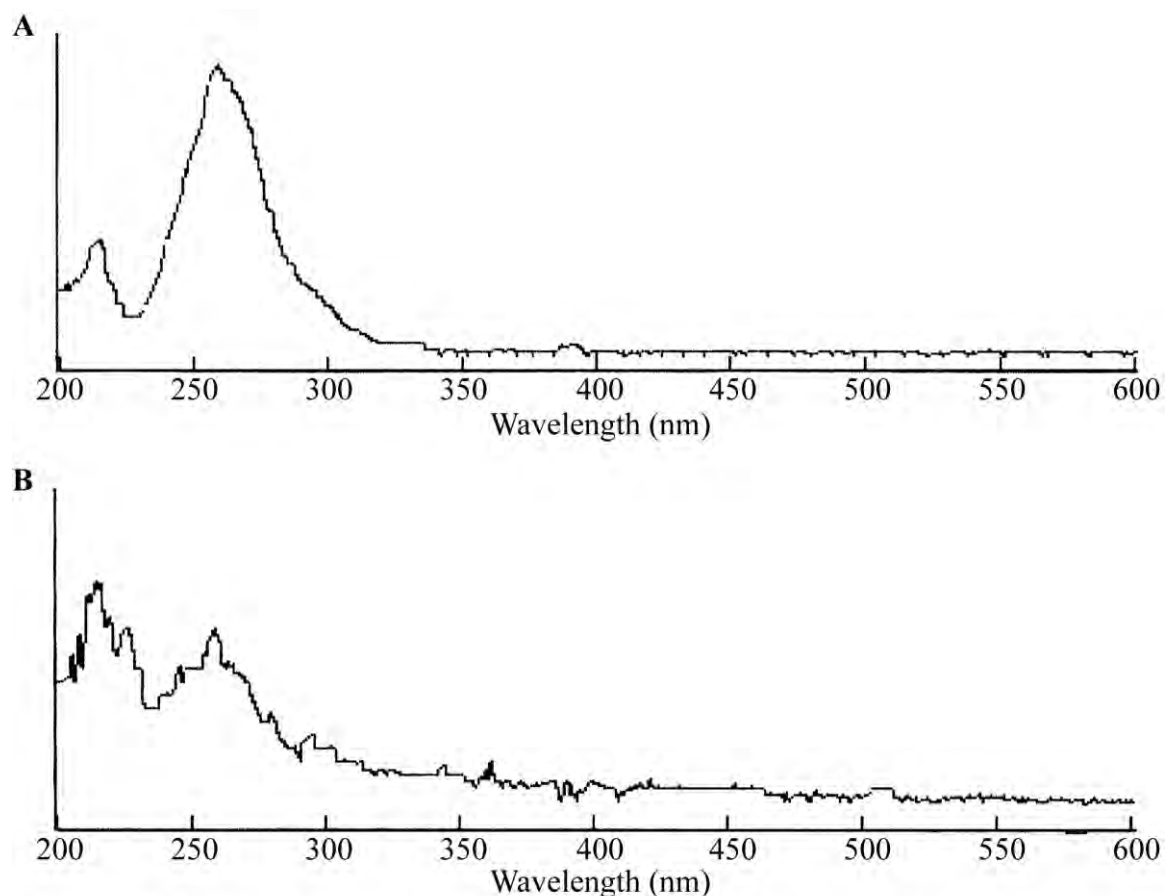


Figure 18. Extended Spectrum Scans of Heated ddH₂O in Microfuge Tubes. The (A) Ambion 12400 microfuge tube, and a (B) VWR 20170-038 microfuge tube with 1.0 mL volumes of ddH₂O were heated at 100 °C, cooled for 2 min in an ice bath, and scanned from 200 nm to 800 nm. In the interest of size and scale, the 600 nm to 800 nm part of the section was removed because it remained consistent with the absorbance observed from 400 nm and higher.

Various stresses imposed on polypropylene plastic tubes result in chemicals migrating into the solutions. Microfuge tubes are subjected to a variety of stresses in the laboratory, which include heating, freezing, high g-force, sonication, autoclaving, and exposure to solvents. We wanted to measure the impact of these stresses on the tubes and to monitor the degree to which the chemical or chemicals migrated out of the plastic. At this point, we have established that heating is one way that the migration is initiated, but

not the specific temperatures needed. To test this, 1 mL of ddH₂O was added to several VWR tubes and they were allowed to stand at RT, or heated to 37, 70, or 100 °C for 30 min in triplicate, and the solutions scanned from 200 nm to 350 nm (Figure 19). At 25 and 37 °C, the pattern began to emerge at a low intensity, but was still distinct.

Curiously, the 258 nm wavelength was where the maxima occurred and reached small, but significant levels around 0.080. Heating to 70 °C yielded a much more intense peak, > 0.110, but with the 258 nm still being the maximum. The 218 nm peak was almost as intense at this temperature. The tubes that were heated to 100 °C had the most intense peaks with the A₂₁₈ reaching 0.250 and higher.

Heating of microfuge tubes is very common in biochemical laboratories.

Experiments are routinely performed in these tubes where they are incubated at 37 °C for lengthy periods of time to perform enzyme-catalyzed reactions. Heating to 70 °C is a common practice as well, which is the optimum for many thermostable enzymes, as well as to inactivate numerous enzymes used in molecular biology. The melting of DNA is performed using 100 °C heat, and is regularly done in these same tubes. It is therefore essential that the presence of the leached substance be accounted for in experiments using UV absorbance to quantify the contents of the tubes after heating. Furthermore, it has been shown that certain substances leached from polypropylene plastic tubes have an inhibitory effect on some classes of enzymes (39). Although our experiments were not concerned with the inhibitory nature of the leachate or any other interfering role that they may play in experiments, it is worthwhile to note their presence and be aware of potential complications.

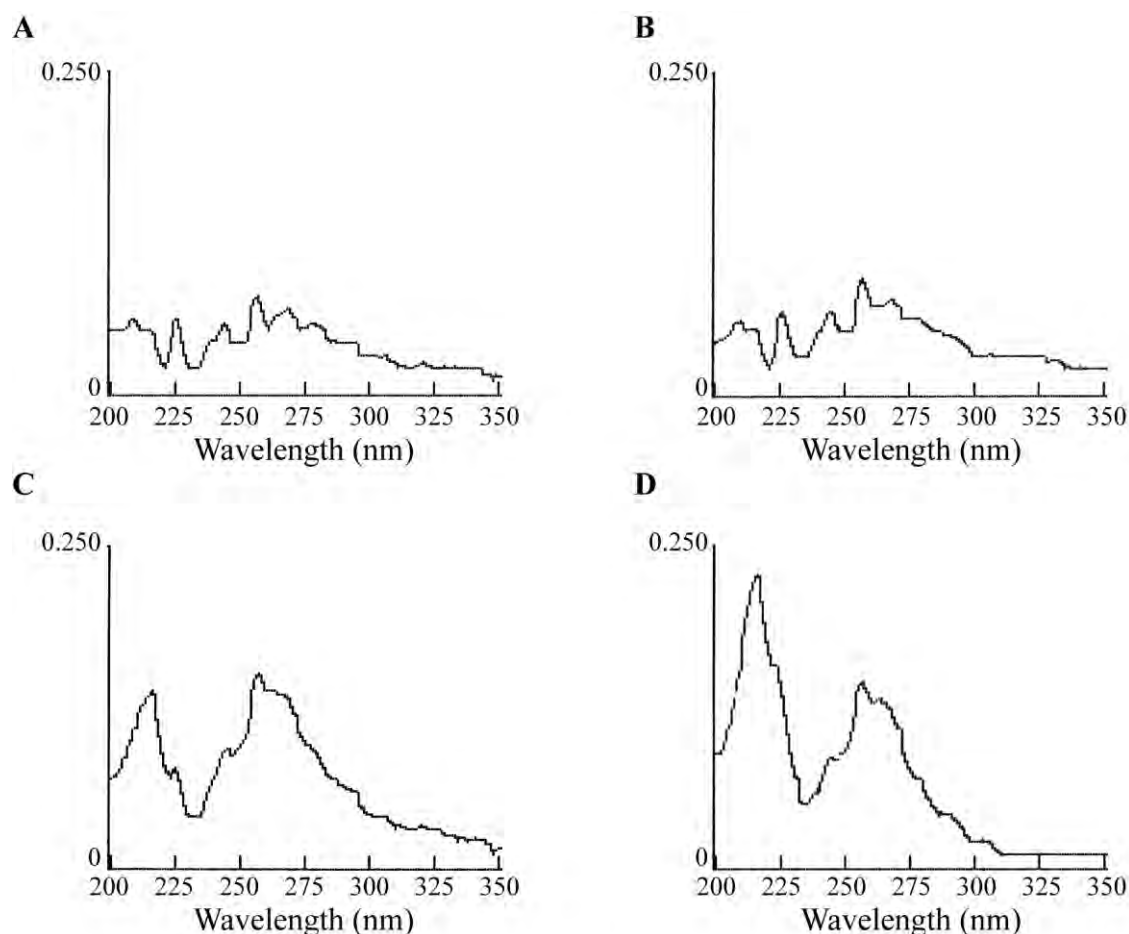


Figure 19. Absorbance Scans of ddH₂O Heated at Various Temperatures in Tubes. Heating temperatures were (A) 25 °C, (B) 37 °C, (C) 70 °C, and (D) 100 °C for 30 min and then allowed to cool to room temperature. All trials used a 1.0 mL volume of ddH₂O in VWR 20170-038 microfuge tubes.

High g-forces will instigate the migration of some leachates. Centrifugation is a method almost universally employed in the laboratory, and the induced high g-forces that are imposed upon the tubes may have some effect on the migration of the leaching species into the solution. Using only ddH₂O in the tubes once again, we centrifuged the tubes in two common centrifuges. The Eppendorf Centrifuge 5415 D was spun at

16,100g and the Beckman Coulter Microfuge 18 Centrifuge was run at the faster rate of 18,000g for 20 min. The tubes were tested in quadruplicate and the supernatant scanned from 200 nm to 350 nm. The resulting scans indicated that the tubes do leach chemicals at a low rate, but the higher g-forces induce more leaching. At 16,000g, the absorption maxima averaged around 0.030 and at the high speed it averaged ~0.050 (scans not shown).

Cavitation and sonic heat induction will promote chromophore leaching.

Sonication is a method that creates heat and high-energy sound waves. In biochemistry it is used to separate or lyse cells, but has also been employed to shear large molecules such as DNA. Sonication is often performed in the microfuge tubes, although for only brief periods of time. To observe the effects of sonication on the tubes, ddH₂O was scanned from 200 nm to 350 nm immediately after being added to the tube (Figure 20). After 5 min of sonication it was scanned again and the pattern observed in previous stress studies of VWR tubes emerged with an average intensity at the highest peak being over 0.110. An additional 5 min of sonication was done to the solution and it was scanned again. The predicted pattern was clearly present and rather intense, with the maximum average absorbance at 0.175. Sonication was clearly facilitating the leaching of the unknown material(s) into the solution, possibly as a result of heating.

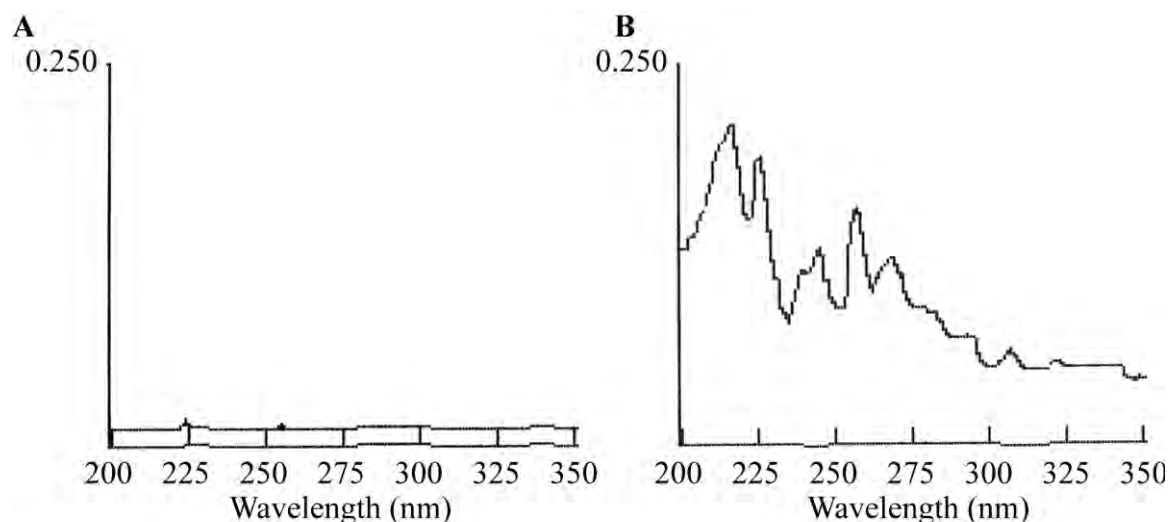


Figure 20. Absorbance Scans of ddH₂O Sonicated in Tubes. UV absorbance spectra of (A) unsonicated ddH₂O and (B) sonicated ddH₂O. Sonication was performed for 5 min and the UV absorbance scan was performed after the solution had been cooled to room temperature.

Sterilizing microfuge tubes in an autoclave will induce leaching. Standard practice in laboratories using microfuge tubes is to first autoclave them to ensure sterilization. Under conditions of high heat (121 °C) and pressure, the microfuge tubes are subjected to a hostile environment that may promote the leaching of the chemicals that have been observed. To test this hypothesis, 10 VWR tubes were placed in a screw top glass jar and covered with 50 mL of ddH₂O. The jar was placed in the autoclave and the machine was run using the liquid cycle. A sample of the water in the jar was taken in triplicate and scanned from 200 nm to 350 nm, which once again showed the signature of the VWR tubes (scans not shown), but at a very intense level, especially for the high volume of water that was used to cover the tubes. The harsh environment of the autoclave was able to get the leachate to readily move out of the polypropylene and into the water, though under normal circumstances the microfuge tubes would not be submerged in

water. They would be autoclaved dry in a container, but the heat and pressure may induce sweating of the leachate to the surface of the tube, which in turn could be easily dissolved into a solution that is placed in the tube.

Chemical leaching is promoted by organic solvents. Organic solvents are routinely used in biochemistry laboratories. These solvents can sometimes be very strong and plastics have been known to be soluble in them. In biochemical laboratories, they are usually used at low concentrations and often mixed with water, but they may still enhance the migratory effect of the leachate into the solution. In order to observe the effects of organic solvents we selected several common chemicals and aliquoted them into the tubes for 30 min, under heat if possible. We opted to use acetone, chloroform, ethanol, diethyl ether, DMSO, and methanol. Some of the more volatile solvents could not withstand heating in the tubes and would vaporize in low heat. The high pressure from the vaporized solvent would force open the tube lids. Therefore, all solvents were allowed to stand either at RT or incubated at 37 °C and for 30 min and about 20 hrs. Due to the nature of some of the solvents used, scans were conducted using a quartz cuvette and solutions had to be poured to and from the microfuge tube so that plastic chemicals from the pipet tips would not leach into the solution. Each solvent from a tube was scanned against a blank of the same solvent that had never come into contact with a plastic material.

The patterns that were observed were consistent with each of the solvents, and as we would predict, the intensity of the peaks increased with longer time and higher

temperatures. Each of the solvents tested were capable of drawing the leachate out of the plastic and into solution (Figure 21).

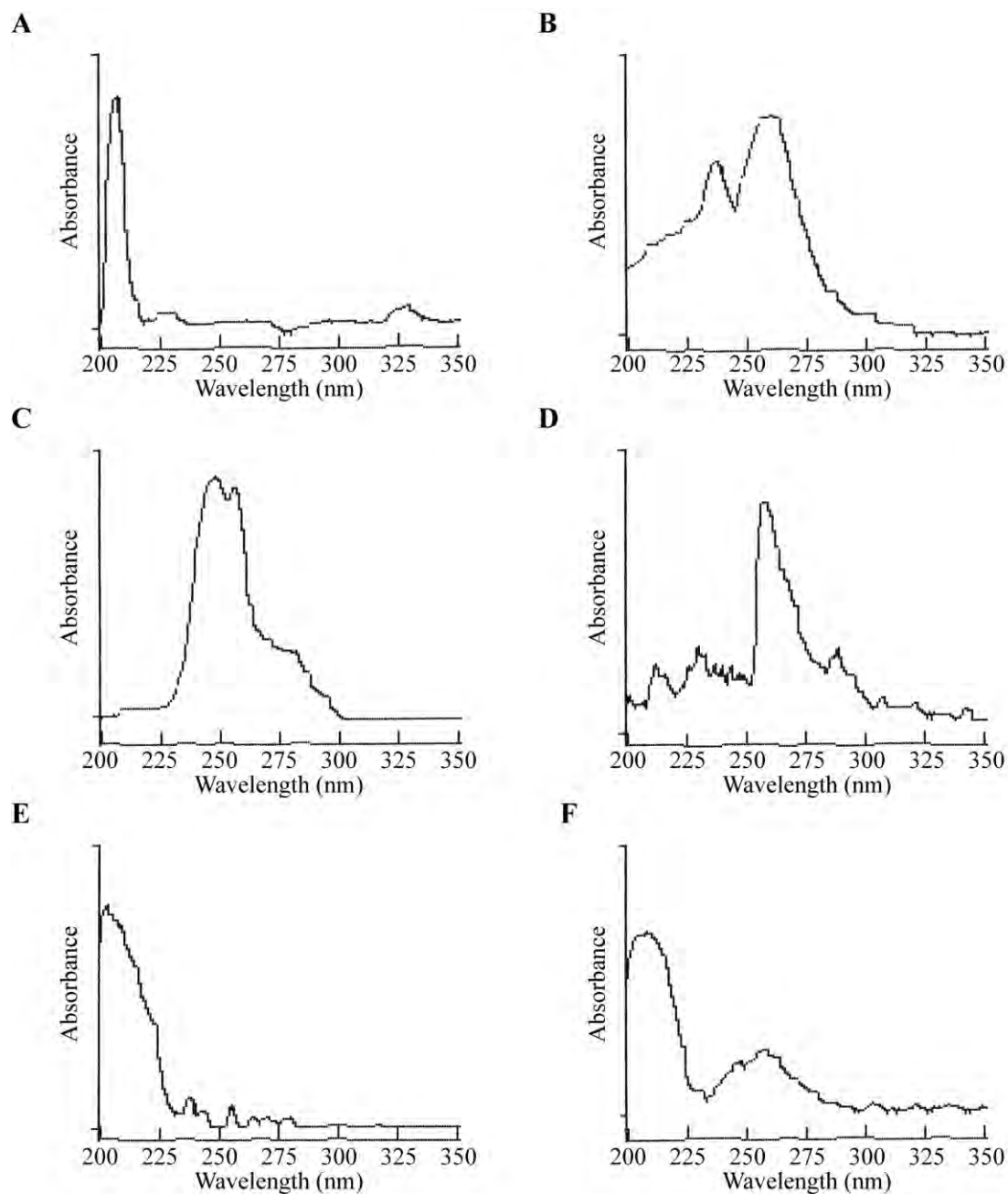


Figure 21. VWR tubes incubated at 37 °C with ~1.0 mL of (A) acetone, (B) chloroform, (C) diethyl ether, (D) dimethyl sulfoxide, (E) ethanol, and (F) methanol.

Heating plastic microfuge tubes induces leaching of additives out of the polypropylene and into the solution, which will absorb UV light at wavelengths of interest to researchers when quantifying biomolecules. In order to test the extent of the interference by the additives in biomolecular assays, we scanned BSA protein and salmon sperm chromosomal protein from 200 nm to 350 nm (Figure 22A, B). The same solutions were then heated at 100 °C for 30 min and scanned again across the same spectrum (Figure 22C, D). The intensity of the absorbance was clearly increased. The absorbance of the BSA protein was increased from 0.404 to 0.586 at its maximum, an increase of almost 50%. Similar results were observed in the salmon sperm chromosomal DNA scans, where the initial absorbance was increased from 0.246 to 0.351 after heating.

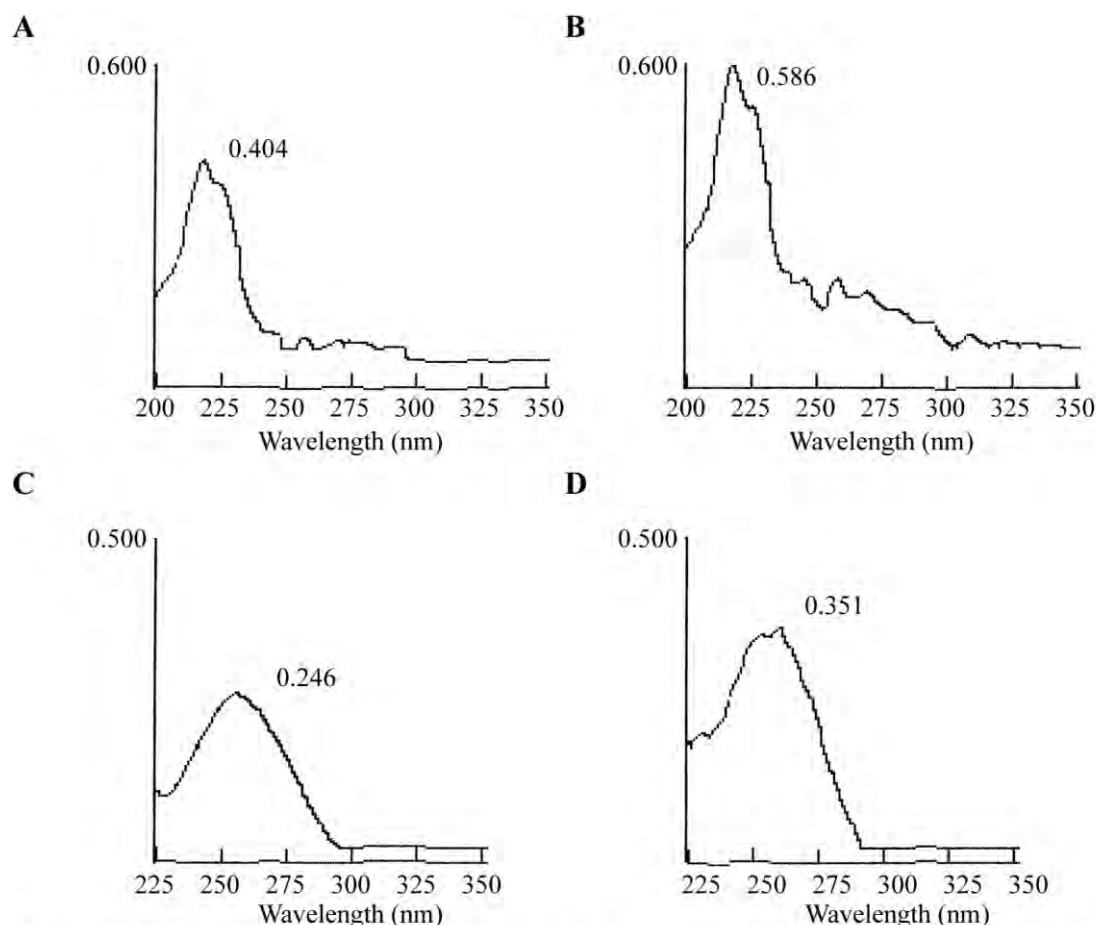


Figure 22. Change in Absorbance of BSA and Salmon Sperm Chromosomal DNA from Heating in Tubes. Absorbance spectra of (A) unheated BSA protein, (B) heated BSA protein, (C) unheated salmon sperm chromosomal DNA (D) and heated salmon sperm chromosomal DNA. The two BSA scans are from the same solution, and the salmon sperm chromosomal DNA scans are from the same solution. Both (B) and (D) were heated for 30 min at 100 °C and cooled in an ice bath before scanning. The numbers above the peaks are the levels of absorbance at each apex.

Thermal cycling using thin-walled polypropylene tubes results in interference with UV absorption. Polymerase Chain Reaction (PCR) is a common biochemical research technique whereby DNA samples are amplified by repetitive cycles of heating and cooling. The solution is heated to almost 100 °C (usually 94-95 °C) to melt the DNA, and cooled in the presence of DNA polymerase primers, which will

anneal to the DNA and allow the polymerase to replicate the sample DNA strand. The polypropylene plastic used in PCR tubes is much thinner as to allow the temperature of the solution to be quickly affected by the PCR machine. Due to manufacturing protocols, the plastic is exposed to very high temperatures in the process of fabrication. To measure the effects of cycling heat and cooling, we tested 3 Gene Mate Ultra Flux Dome Cap PCR tubes C-3257-1 from ISC Bio Express by subjecting the tubes to 30 cycles using the following parameters: 95 °C for 2 min, followed by 30 cycles involving 95 °C for 45 sec, 60 °C for 30 sec, 72 °C for 2 min. The tubes were then incubated at 72 °C for 7 min and placed at 4 °C until removed from the cycler. Each tube was then scanned from 200 nm to 350 nm (Figure 23). The peak absorbances ranged from ~0.050 and 0.100 at around the 220 nm wavelength, but there was still a notable contribution to absorbance at the 260 nm wavelength that was around 2/3 the intensity of the peak.

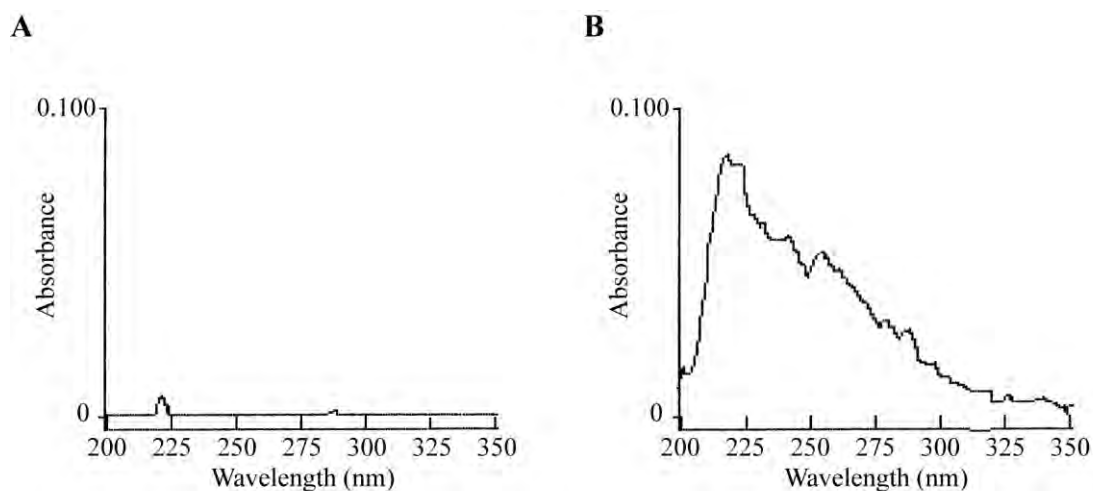


Figure 23. Absorbance Scans of ddH₂O After Thermocycling in PCR Tubes. ddH₂O in ISC Bio Express PCR tubes was scanned (A) before cycling and (B) after 30 cycles in the PCR machine.

Researchers who use heat when performing experiments on biomolecules must be aware of the changes to the absorbance of the solution when using UV light. The additives that migrate into the solution may skew measurements and result in improper quantification of the biomolecule of interest. Many methods common to biochemistry laboratories will cause this to happen, and efforts to minimize this effect should be taken. The Axygen MCT-150-C, a newer model of microfuge tube, advertises that fewer additives are used in the molding process and that it incorporates a “diamond boring” process that eliminates the need for mold release agents that can interfere with UV absorbance readings. This tube produced the smallest leachate of any of the tubes tested (Figure 24I), with essentially no detectable UV absorbance between 200-300 nm using the standard assay (30 min, 100 OC). Only on other tube, the Eppendorf 245107 microtube, produced such a clean scan (Figure 24J).

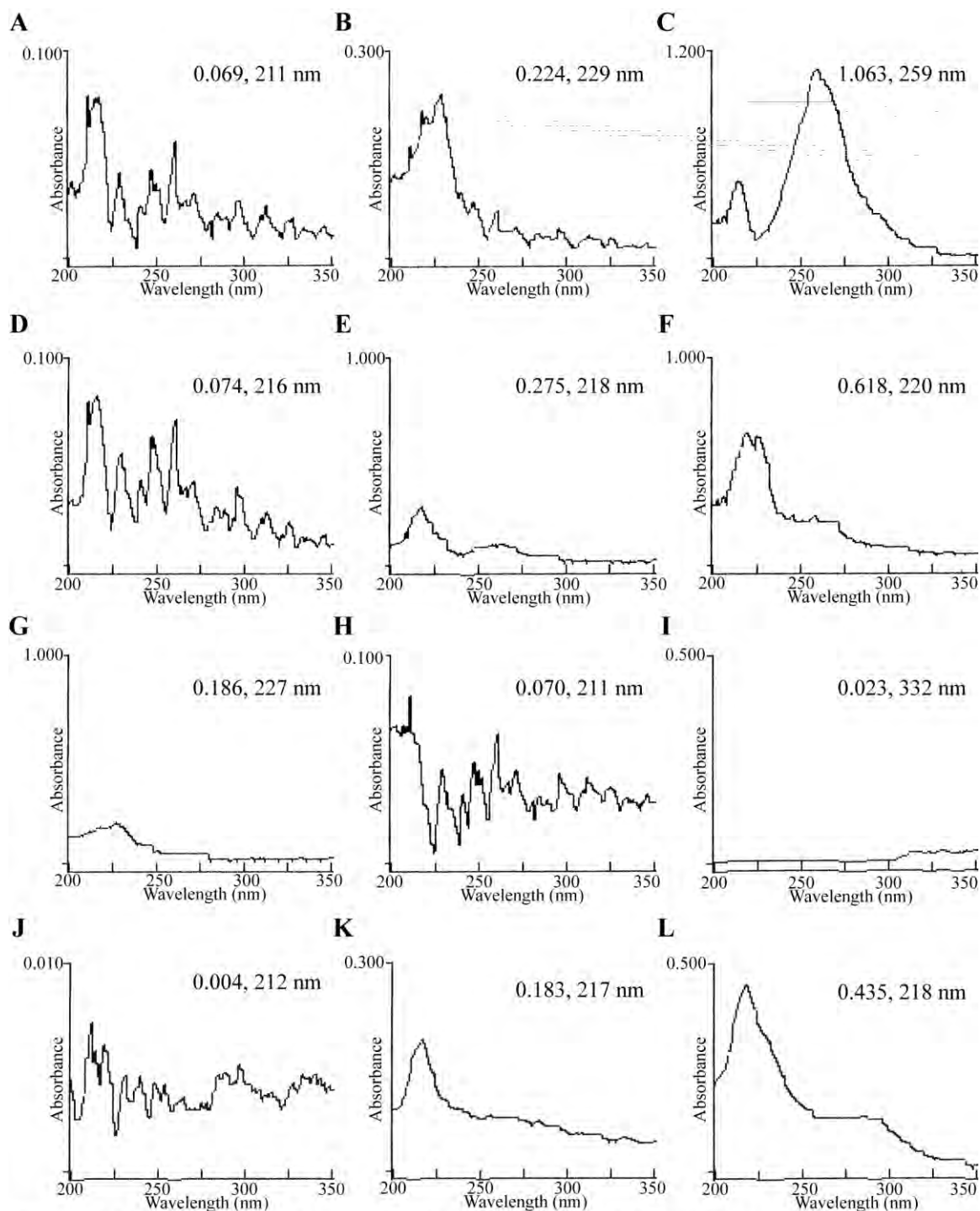


Figure 24. Scans of ddH₂O Heated in Various Brands of Tubes. Scanned after 100 °C for 30 min in (A) Gene Mate PCR tube C-3257-1, (B) Ambion AM 12300, (C) Ambion AM 12400, (D) Axygen MCT-175-A, (E) VWR 20170-038 (old bag), (F) VWR 20170-038 (new bag), (G) ISC Bio Express C-3261-3, (H) Ambion AM 12425 (I) Axygen MCT-150-C, (J) Eppendorf 245107, (K) Fisherbrand 02-681-376, (L) Sarstedt 72.694.

SUMMARY & CONCLUSIONS

Research into aqueous suspensions of both Na-Mont and Ca-Mont has characterized the contributions to UV light absorbance and its relationship to tactoid dispersion. Monitoring the extent to which various factors promote sedimentation and increase adsorption of polymers to clay platelets have led to the development of an improved assay for the quantification of bound single-stranded DNA. By accounting for the contribution of unpelleted clay and optimizing the conditions under which polymers and biomolecules adsorb to the surface of the platelets, this assay methodology should translate to other studies involving the interaction of clay with biopolymers and organic molecules.

Our work investigating the dispersion characteristics of clay tactoids by heat and sonication was performed primarily using 1.5 mL microfuge tubes. The stresses imposed on the tubes in the course of this research demonstrated that chemicals are released into aqueous solutions that absorb UV light. These leachates exhibit strong absorption in regions of the spectrum that correspond to the DNA and protein peak maxima. We have shown that leaching increases in conjunction with procedures that cause heating of the tubes, such as incubation, sonication, and centrifugation. Temperatures equal to or greater than 37 °C draw these chemicals out of the polypropylene, with higher temperatures causing more leaching, which in turn lead to more interference with measurements involving UV spectroscopy.

It has recently been reported that two additives released from some commercial microfuge tubes, the slip agent oleamide and the biocide DiHEMA, inhibit the enzyme human monoamine oxidase-B (hMAO-B) and may also bind to γ -aminobutyric acid type A (GABA_A) receptor proteins (McDonald, et al. 2008). Those results demonstrate that leachates may interfere with functional assays for some proteins, but our observations suggest that a more widespread problem exists.

Common biochemical practices involve spectrophotometric measurement of light absorbance by biomolecules. Molecular biology laboratories employ the absorbance at 260 nm to quantify DNA and 220 nm and 280 nm to detect proteins. Additionally, samples are frequently heated at elevated temperatures to accelerate enzyme-catalyzed reactions, lyse cells, denature DNA, and inactivate enzymes. These procedures stimulate the release of UV-absorbing polypropylene leachates. Leaching of UV absorbing species was observed almost universally across all brands of microfuge tubes, and given the ubiquitous nature of leaching, it is probable that many past studies that involve UV spectroscopy have been subject to error. The degree of error is difficult to estimate, but can be substantial. The magnitude of absorbance typical of chemicals leached from a microfuge tube is up to 1.0 to 2.0 absorbance units, though it has been observed to be much higher. Inconsistencies occur in the level of interference among tubes of the same brand that come from different batches. Other factors to account for is the wavelength that was employed and heating method used, as this will influence the degree to which the measurements were skewed. It is our recommendation that future studies use microfuge tubes that were polymerized using minimal amounts of chromophoric

additives and slip agents, have high temperature stability, as well as being diamond-polished molds because it involves no chemicals.

REFERENCES

1. Bernal, J. D. *Proc. R. Soc. London, A* **1949**, 62, 537-558.
2. Ferris, J. P. *Elements* **2005**, 1, 145-149.
3. Gallori, E.; Bazzicalupo, M.; Canto, L. D.; Fani, R.; Nannipierri, P.; Vettori, C.; Stotzky, G. *FEMS Microbiol. Ecol.* **1994**, 15, 119-126.
4. Cai, P.; Huang, Q.; Chen, W.; Zhang, D.; Wang, K.; Jiang, D.; Liang, W. *Soil Biol. & Biochem.* **2007**, 39, 1007-1013.
5. Khanna, M.; Stotzky, G. *Appl. Environ. Microbiol.* **1992**, 58, 1930-1939.
6. Paget, E.; Monrozier, L. J.; Simonet, P.; *FEMS Microbiol. Lett.* **1992**, 97, 31-40.
7. Stotzky, G. *Gene Transfer Among Bacteria in Soil*; McGraw Hill Book Co.: New York, NY, 1989.
8. Pinnavaia, T. J.; Beall, G. W. *Polymer-Clay Nanocomposites*; Wiley Press: Hoboken, NJ, 2000.
9. Coveney, P. V.; Evans, J.; Whiting, A. Research grant, Centre for Computational Research, London, UK, 2006.
10. Carretero, M. I. *Appl. Clay Sci.* **2002**, 21, 155-163.
11. Choy, J. H.; Choi S. J.; Oh, J. M.; Park, T. *Appl. Clay Sci.* **2007**, 36, 122-132.
12. Chen, B. *Br. Ceram. Trans.* **2004**, 103, 241-249.
13. Carrado, K. A. *Appl. Clay Sci.* **2000**, 17, 1-23.
14. Schramm, L. L.; Kwak, J. C. T. *Clays Clay Miner.* **1982**, 30, 40-48. Whalley, W. R.; Mullins, C. E. *Clay Miner.* **1991**, 26, 11-17.
15. Chen, Y.; Shaked, D.; Banin, A. *Clay Miner.* **1979**, 14, 93-102.

16. Banin, A.; Lahav, N. *Nature* **1968**, 217, 1146-1147.
17. Yariv, S.; Lapidés, I. *Clays Clay Miner.* **2003**, 51, 23-32.
18. Lubetkin, S. D.; Middleton, S. R.; Ottewill, R. H. *Philos. Trans. R. Soc. London, A* **1984**, 311, 353-368.
19. Frenkel, H.; Shainberg, I. *J. Soil Sci.* **1981**, 32, 237-246.
20. Vaia, R. A.; Jandt, K. D.; Kramer, E. J.; Giannelis, E. P. *Chem. Mater.* **1996**, 2628-2635.
21. Poly, F.; Chenu, C.; Simonet, P.; Rouiller, J.; Monrozier, L. J. *Langmuir* **2000**, 16, 1233-1238.
22. Cai, P.; Huang, Q.; Zhang, X. *Appl. Clay Sci.* **2006**, 32, 147-152.
23. Banin, A.; Lawless, J. G.; Mazzurco, J.; Church, F. M.; Margulies, L.; Orenberg, J. B. *Orig. Life Evol. Biosph.* **1985**, 15, 89-101.
24. Franchi, M.; Ferris, J. P.; Gallori, E. *Orig. Life Evol. Biosph.* **2003**, 33, 1-16.
25. Ferris, J. P.; Gozen, E.; Agarwal, V. K. *Orig. Life Evol. Biosph.* **1989**, 19, 153-164.
26. Pietramellara, G.; Franchi, M.; Gallori, E. *Biol. Fert. Soils* **2001**, 33, 402-409.
27. Sushko, M. L.; Shluger, A. L.; Rivetti, C. *Langmuir* **2006**, 22, 7678-7688.
28. Ferris, J. P. *Orig. Life Evol. Biosph.* **2002**, 32, 311-332.
29. Franchi, M.; Bramanti, B.; Bonzi, L. M.; Orioli, P. L.; Vettori, C.; Gallori, E. *Orig. Life Evol. Biosph.* **1999**, 29, 297-315.
30. Mao, Y.; Daniel, L. N.; Whittaker, N.; Saffiotti, U. *Environ. Health Perspect.* **1994**, 102, 165-171.
31. Cai, P.; Huang, Q.; Zhu, J.; Jiang, D.; Zhou, X.; Rong, X.; Liang, W. *Colloids Surf., B* **2007**, 54, 53-59.
32. Kawase, M.; Hayashi, Y.; Kinoshita, F.; Yamato, E.; Miyazaki, J. I.; Yamakawa, J.; Ishida, T.; Tamura, M.; Yagi, K. *Biol. Pharm. Bull.* **2004**, 27, 2049-2051.
33. Lin, F. H.; Chen, C. H.; Cheng, W. T. K.; Kuo, T. F. *Biomaterials* **2006**, 27, 3333-3338.

34. Khanna, M.; Yoder, M.; Calamai, L. *Sci. Soils* **1998**, 3, 1-10.
35. Oehlmann, J.; Oetken, M.; Schulte-Oehlmann, U. *Environ. Res.* **2008**, 108, 140-149.
36. Shotyk, W.; Krachler, M.; Chen, B. *J. Environ. Monit.* **2006**, 8, 288-292.
37. Marcato, B.; Guerra, S.; Vianello, M.; Scalia, S. *Int. J. Pharm.* **2003**, 257, 217-225.
38. McDonald, G. R.; Hudson, A. L.; Dunn, S. M. J.; You, H.; Baker, G. B.; Whittal, R. M.; Martin, J. W.; Jha, A.; Edmonson, D. E.; Holt, A. *Science* **2008**, 322, 917.
39. Vandenberg, L. N.; Maffini, M. V.; Sonnenshein, C.; Rubin, B. S.; Soto, A. M. *Endocrinology* **2009**, 30, 75-95.
40. Beall, G. W.; Sowersby, D. S.; Roberts, R. D.; Robson, M. H.; Lewis, L. K. *Biomacromolecules* **2009**, 10, 105-112.
41. Sambrook, J.; Russell, D. W. *Molecular Cloning: A Laboratory Manual. 3rd Edition*; Cold Spring Harbor Laboratory Press: Cold Spring Harbor, NY, 2001.
42. Beall, G. W.; Goss, M. *Appl. Clay Sci.* **2004**, 27, 179-186.
43. Rappe, A. K.; Goddard, W. A. III. *J. Phys. Chem.* **1991**, 95, 3358-3363.
44. Zhang, C; van der Maarel, J. R. C. *J. Phys. Chem., B* **2008**, 112, 3552-3557.

VITA

Michael Harrison Robson was born on July, 14th 1978 in Tucson, Arizona to William Michael Robson and Penni Marie Robson. He was raised in the American Southwest, growing up in Arizona and New Mexico. He attended high school in Albuquerque at La Cueva H.S. and spent 3 years attending Colorado State University, and transferred to the University of Arizona where he received a Bachelor of Science in Molecular and Cellular Biology. He is receiving his Master's of Science from Texas State University-San Marcos in August, 2009 and will be pursuing his Ph.D. in Engineering from the University of New Mexico in Nanoscience and Microsystems. He courted and ultimately married the fetching, young Lacie DeLynn Ledford on November 24, 2007 and are expecting their first born child on January 16th, 2010.

Permanent Address: mhrobson@hotmail.com

This thesis was typed by Michael H. Robson.